

QCD and Theory of Hadrons

Yu.A.Simonov

State Research Center

Institute of Theoretical and Experimental Physics,
Moscow, Russia

Abstract

Nonperturbative QCD approach is systematically derived starting from the QCD Lagrangian. Treating spin effects as a perturbation, one obtains the universal effective Hamiltonian describing mesons, hybrids and glueballs.

Constituent mass of quark and gluon is calculated via string tension. The resulting spectrum of mesons, hybrids and glueballs obtained is in good overall agreement with lattice data and experiment.

Contents

1. Introduction.
2. The QCD vacuum, confinement and chiral symmetry breaking.
3. Perturbative and nonperturbative field configurations. Asymptotic freedom and infrared freezing.
4. Background perturbation theory and definition of hadron states.
5. Relativistic path integrals and relativistic Hamiltonians.
6. Spectrum of light mesons, hybrids and glueballs. Regge trajectories.
7. Light-cone Hamiltonian and spectra for mesons.
8. Conclusions.

1 Introduction

Hadron physics is a well-established field with enormous experimental treasury of facts; on the theoretical side there are different models, some of these are well developed and have an impressive predicting power. The theoretical situation cannot be however considered satisfactory, taking into account that it is now clear that QCD is the real theory of strong interactions and

can be used for selfconsistent construction of the hadron theory. In addition to that new powerful methods in lattice simulations of QCD yield detailed information not only about spectrum of hadrons, but now also about scattering and hadronic matrix elements.

The reason for this discrepancy was lack of analytic nonperturbative (NP) methods in QCD, which could be used for systematic derivation of QCD-based models. Recently the situation started to improve, and new powerful analytic approaches have been suggested and checked versus experiment and lattice data. Remarkably many of the previous model results are derived now by these approaches in a rather direct way from the first principles, i.e. from the QCD Lagrangian, and it is gratifying that these features are supported by experiment and lattice data. In addition new NP methods allow to resolve old problems, which plagued existing models. The (incomplete) list of problems includes:

1) The problem of Regge slope. Relativistic quark models (RQM) predict for it the value $(8\sigma)^{-1}$, where σ is the string tension, while the string models give $(2\pi\sigma)^{-1}$, which seems more realistic from physical point of view.

2) The problem of Regge intercept. Both RQM and string models predict too high values for the hadron masses, which is mended by introduction of large negative constant in the Hamiltonian, of unknown dynamical origin.

3) Perhaps a more fundamental problem is the problem of constituent mass of quarks and gluons. The latter are introduced as a phenomenological input to reproduce spectrum and static characteristics and are different in the relativistic and nonrelativistic versions of the model. The dynamical origin of constituent masses is unknown.

4) The problem of quark radius and formfactors. In RQM (to take a most developed model) radius of hadrons comes out to be too small which is usually mended by introduction of some effective quark radius, the origin of this radius is not understood.

5) A very fundamental problem which lies at the basis of the whole QCD, is the connection between the quark models of hadrons (based on the minimal number of degrees of freedom – those of valence quarks and gluons) and high–energy scattering, including DIS, where bare (current) quark degrees of freedom enter, including quark sea and gluon d.o.f. As an example, about one half of energy–momentum is transported by a gluon cloud around proton, while in the constituent quark model this gluon cloud is not evident.

In this review we attempt to establish a basis for answering these questions, using new NP approaches in QCD. These include: 1) a new background field theory, where NP fields play role of the background, and the separation of perturbative and NP is made formally exact by virtue of the 'tHooft identity; 2) Relativistic path integral representation for quark and gluon Green's functions; 3) Method of relativistic Hamiltonians with auxiliary functions; 4) A very recent method of effective contour–dependent quark Lagrangians, yielding a simple picture of hadrons in the large N_c limit.

The space limits of this review leave out many details of the formalism, which can be found in the original literature. Moreover a very important part of the hadron physics – the strong hadron decays – is left over completely for future.

2 The QCD vacuum, confinement and chiral symmetry breaking (CSB)

QCD is believed to be the theory of strong interaction. The evidence for that statement comes from comparison of perturbative QCD and the so-called QCD-motivated models with experiment and also from lattice data.

There is some gap between models, treating nonperturbative (NP) features of QCD, and QCD Lagrangian, which is now filled in by new NP methods and Monte-Carlo calculations. It is the purpose of the present review to describe these new NP methods, confronting their results with experiment and lattice data, thus demonstrating that one can indeed derive theory of hadrons from the first principles of QCD with few assumptions, which can be checked independently.

To describe properties of the QCD vacuum and NP dynamics of quarks and gluons one must consider the Euclidean QCD Lagrangian (since NP configurations turn out to be Euclidean) and the QCD partition function has the following form.

$$Z = \int DAD\psi D\psi^+ \exp[L_0 + L_1 + L_{\text{int}}] \quad (1)$$

where we are using Euclidean metric and define

$$L_0 = -\frac{1}{4} \int d^4x (F_{\mu\nu}^a)^2, \quad (2)$$

$$L_1 = -i \int {}^f\psi^+(x) (\hat{\partial} + m_f) {}^f\psi(x) d^4x, \quad (3)$$

$$L_{\text{int}} = \int {}^f\psi^+(x) g \hat{A}(x) {}^f\psi(x) d^4x. \quad (4)$$

Here and in what follows ${}^f\psi_{a\alpha}$ denotes quark operator with flavour f , color a and bispinor index α .

The quantum theory of QCD is believed to be fixed by equations (1-4) and one prescribed scale, e.g. Λ_{QCD} .

There are two main features of NP QCD, which make our world and ourselves as we are: confinement and CSB.

Confinement is a property of gluonic part of Lagrangian (2) (for a review see [1]) and most easily defined for static quark Q and antiquark \bar{Q} neglecting light quarks, in which case the celebrated order parameter is the Wilson loop (to be often used below),

$$\langle W(C) \rangle = \int DA \exp L_0 \cdot P \exp i g \int_C A_\mu dz_\mu. \quad (5)$$

We suppress here the gauge fixing and ghost terms for simplicity. For large contours C one has Wilson criterium of confinement [1]

$$\langle W(C) \rangle = \exp(-\sigma S - \gamma P) \quad (6)$$

where S is the minimal area inside contour C and σ is the string tension, while P is the perimeter of the loop C . Note that theory must connect σ and Λ_{QCD} – the only scale of QCD, how it is done on the lattice and in some models – see in [2].

Confinement in the form of area law (6) produces linear potential for heavy quark and anti-quark at large distances, $V_{Q\bar{Q}}^{(C)}(R) = \sigma R$, and in section 5 we shall find also other contributions to $V_{Q\bar{Q}}(R)$ due to perturbative gluon exchanges and spin-dependent parts. It is important that light-quark loop contributions are suppressed by powers of $1/N_c$ and can be accounted for perturbatively.

Whereas confinement enters directly via $W(C)$ in the heavy quark Green's function (see section 5), it is much more involved problem for light quarks, especially for quarks in pions, since their Green's function cannot be expressed readily through $W(C)$. Physically this fact is connected to the Zitterbewegung of light quark which is connected to the phenomenon of chiral symmetry breaking. To proceed one remarks that massless quarks can be split into left and right chiral parts, $\Psi(x) = \Psi_R + \Psi_L$ and Ψ_R, Ψ_L enter Lagrangians (3) and (4) in the additive way, exemplifying the chiral symmetry of the group $U_L(N_f) \otimes U_R(N_f)$. It was shown in [3], that nonperturbative gluonic fields responsible for confinement, also produce CSB for light (massless) quarks. Concretely the appearance of the string (which transforms as Lorentz scalar) for a light quark is already a sign of spontaneous CSB, and the string appears as a solution of the nonlinear equation for the light-quark Green's function [3].

For most mesons, however, not pions and kaons, chiral and spin effects can be treated as perturbation of the basic confinement dynamics. The corresponding Hamiltonian [4,5] looks much simpler, and reduces in some limiting cases to the familiar relativistic potential models [6,7,8]. We derive these Hamiltonians in section 5 in the c.m. system.

Of special interest in modern hadron spectroscopy are glueballs and hybrids. Here relativistic hamiltonians can be easily generalized to include gluon degrees of freedom, if gluon spin interaction is considered as perturbation. The spectrum obtained in this way is discussed in section 6 and is in good agreement with lattice data. One should note, that nowhere in our formalism we introduce constituent quark or gluon mass, and the only input mass parameters are string tension σ , and Λ_{QCD} (in addition to current quark masses m_f , renormalized at the scale $1GeV$). With such input one obtains a wide variety of hadron states and its properties in good overall agreement with experiment and lattice data. We also define and calculate the constituent mass of quark and gluon in terms of σ .

3 Perturbative and nonperturbative field configurations

One of basic mysteries of QCD is the fact, that gluon field plays two different roles:

- a) gluons are propagating, and at small distances this process can be described perturbatively, leading in particular to color Coulomb interaction between quarks (antiquarks);
- b) gluons form a kind of condensate, which serves as a background for the propagating perturbative gluons and quarks. This background is Euclidean and ensures phenomena of confinement and CSB.

Correspondingly we shall separate the total gluonic field A_μ into perturbative part a_μ and nonperturbative (NP) background B_μ :

$$A_\mu = B_\mu + a_\mu \tag{7}$$

There are many questions about this separation, which may be answered now only partially, e.g. what exactly is the criterion of separation. Possible answer is that perturbative fields a_μ get their dimension from distance (momentum), and therefore all correlators of fields a_μ (in absence

of B_μ) are singular and made of inverse powers of $(x-y)$ and logarithms, where enters the only dimensional parameter of perturbative QCD – Λ_{QCD} . Therefore evidently any dimensionful constant, like hadronic masses or string tension cannot be obtained as a perturbation series. In contrast to that, NP fields B_μ have mass dimension due to the violation of scale invariance which is intrinsically present in the gluodynamics Lagrangian. The origin of separation (7) is clearly seen in the solutions of nonlinear equations for field correlators [9]: a perturbative solution of those leads to singular power-like field correlator, whereas at large distances there is a selfconsistent solution of the equations, decaying exponentially with distance with arbitrary mass scale, since equations in [9] are scale-invariant. Full solution including intermediate distances produces mixed perturbative–nonperturbative terms, containing both inverse powers of distance and exponentials. For these terms criterion of separation fails.

One can avoid formally the question of separation principle (and of double counting) using t’Hooft identity [10], which allows to integrate in (1) independently over B_μ and a_μ :

$$Z = \frac{1}{N'} \int DB_\mu \eta(B) D\psi D\bar{\psi} Da_\mu e^{L(B+a)} \quad (8)$$

Here $L(A) = L_0 + L_1 + L_{int}$, and A_μ is taken to be $B_\mu + a_\mu$. For the exact formalism starting from (8) we refer the reader to [11,12,2], and here we only quote the form of background propagator $G_{\mu\nu}$ of the gluon, which is found from $L(B+a)$ and will be used in what follows,

$$G_{\mu\nu} = (D_\lambda^2 \delta_{\mu\nu} + 2igF_{\mu\nu})^{-1} \quad (9)$$

where $D_\lambda = \partial_\lambda - igB_\lambda$, and $F_{\mu\nu} = \partial_\mu B_\nu - \partial_\nu B_\mu - ig[B_\mu, B_\nu]$. Neglecting NP background one calculates the perturbative static potential defined gauge-invariantly as

$$V(r) = -\frac{1}{T} \lim_{T \rightarrow \infty} \ln W(r, T) \quad (10)$$

Recent two-loop result in configuration space is [13]

$$V(r) = -C_F \frac{\alpha_R(1/r)}{r}, \quad (11)$$

and in momentum space one has [13]

$$V(q) = -C_F \frac{4\pi\alpha_V(q)}{q^2} \quad (12)$$

with

$$\alpha_V(q) = \alpha_{\bar{M}\bar{S}}(q)(1 + a_1\alpha_{\bar{M}\bar{S}}(q) + a_2\alpha_{\bar{M}\bar{S}}^2) \quad (13)$$

and for the potential in position space one has [13,14]

$$\alpha_R(1/r) = \alpha_{\bar{M}\bar{S}}(1/r)[1 + c_1\alpha_{\bar{M}\bar{S}}(1/r) + c_2\alpha_{\bar{M}\bar{S}}^2] \quad (14)$$

where in quenched QCD ($n_f = 0$) one has

$$c_1 = 1.832, \quad c_2 = 1.758 \quad (15)$$

Employing the lattice measurement of $\alpha(1/r)$ in one obtains [13,14]

$$\Lambda_{\bar{M}\bar{S}}^{(0)} = 0.602/r_0, \quad r_0 \approx 0.5 fm. \quad (16)$$

With this value of Λ_R one obtains the renormalized $\alpha_R(1/r)$ which diverges at the Landau ghost pole, situated at $r \cong 0.2fm$.

Thus the perturbative potential is unacceptable in this form at $r \gtrsim 0.2fm$. However analysis of lattice data in [14,15] reveals, that Landau ghost pole is absent in the data. Potential models usually postulate saturating behaviour of α_R at large r of the type [7]

$$\alpha_R(1/r) = \begin{cases} \alpha_R(\text{one-loop}), & r < r_0 \\ \text{const} = \alpha_R(r_0), & r \geq r_0 \end{cases} \quad (17)$$

In this way one introduces a new parameter $\alpha_R(\text{max}) = \alpha_R(r_0)$, usually chosen around 0.4.

Recently the physical mechanism producing freezing of α_R at large distances was identified in [11,12]. It is connected to the fact, that in the confining background gluons cannot propagate very far from the sources, and typically this distance is inversely proportional to the corresponding hybrid excitation energy (which is of the order of $1.0 \div 1.2GeV$).

At large N_c and in the Euclidean region, $q^2 > 0$, one can predict this saturation (freezing) of α_s theoretically to one loop as [12]

$$\alpha(q) = \frac{4\pi}{\psi\left(\frac{q^2+M_0^2}{m^2}\right) + \ln\frac{m^2}{\Lambda^2}} \quad (18)$$

where ψ is the Euler function, $\psi(z) = \Gamma'(z)/\Gamma(z)$, m^2 is the scale of radial excited states at large n

$$M_n^2 = nm^2 + M_0^2 \quad (19)$$

and M_0^2 the lowest mass state in the channel.

When the argument of ψ function is large, one has asymptotic representation

$$\psi(z) = \ln z - \frac{1}{2z} - \sum_{k=1}^{\infty} \frac{B_{2k}}{2kz^{2k}} \quad (20)$$

Correspondingly $\alpha(q)$ asymptotically assumes the form

$$\alpha^{(as)}(q) = \frac{4\pi}{b_0 \ln \frac{q^2+M_0^2}{\Lambda^2}}, \quad b_0 = \frac{11}{3}N_c - \frac{2}{3}n_f \quad (21)$$

A naive "explanation" of (21) is that gluon acquires the mass $M_0 = m_g$ which eliminates Landau ghost pole.

In reality gluon does not have the mass (this would violate gauge invariance and render the theory nonrenormalizable), but due to confinement is connected by the string to the quarks and this creates the mass of the whole system – the hybrid.

The two-loop asymptotic form of α in the position space looks like [2,12]

$$\alpha_R(1/r) = \frac{4\pi}{b_0 \ln a(r)} \left\{ 1 + \frac{b_1 \ln \ln a(r)}{b_0 \ln a(r)} \right\}^{-1} \quad (22)$$

where $a(r) \equiv \frac{M_0^2+r^{-2}}{\Lambda_R^2}$, and $b_1 = 102$.

Note that the combination $M_0^2 + q^2, M_0^2 + 1/r^2$ in a is the renormalization group (RG), invariant, since both external momenta and background fields (gB_μ), defining M_0 are RG invariant [2,12] (while g and B_μ separately are not).

There are many phenomenological arguments in favour of freezing of α_s at large distances, for a review see [16] and more recent discussion in [12]. A different approach to the freezing behaviour, based on some assumed analytic properties of α has been suggested in [17].

Summarizing phenomenological situation one can state that all known facts are supporting saturating α in Euclidian region at the level $\alpha(max) \leq 0.8$.

Recent lattice data allow a more direct computation of $\alpha(1/r)$ and thereby the freezing phenomenon. In [18] the form (22) was used for α_F , entering the force between static quarks (which is easier to measure on the lattice)

$$F(r) = \frac{4}{3} \frac{\alpha_F(r)}{r^2} \quad (23)$$

The lattice measurements of [15] are compared in Fig.1 of [18] to the theoretical curve (23) with $M_0 = 1GeV$ and $\Lambda_R = 280MeV$. One can see there a good agreement, whereas the nonfreezing behaviour ($M_0 = 0$) clearly contradicts data at $r \geq 0.4fm$.

As one can see from [18], lattice calculations give a clear direct evidence for the freezing of the coupling constant, with the maximal value

$$\alpha^{Lattice}(max) \leq 0.5 \quad (24)$$

A recent experimental evidence for freezing of α_s was found in the detailed analysis of charmonium spectra in [19].

At this point it should be noted that freezing (saturation) is a property of Euclidean (space-like) interactions. In the timelike region ($q^2 < 0$) Equation (12) yields complex logarithm, which is drastically important for time-like formfactors and Drell–Yan processes. From physical point of view logarithmic branch points of α_s are not relevant, and the analytic structure of α_s is better displayed by the Equation (18) valid in the large N_c limit. In this limit all singularities of physical amplitudes are poles, and in the physical scheme of α_s renormalization, when α_s is directly connected to some physical amplitude, α_s should have only poles, which are clearly displayed in (18). At large $|q^2|$, $q^2 \gg m^2$, one can average over many poles and return to the complex logarithmic dependence in (12), in approximate agreement with standard α_s expression, where $M_0^2 \equiv 0$.

So far we explored purely perturbative expressions for static potential or modified due to the NP background. Now we turn to the purely NP static interaction, i.e. to the confining potential. To this end one rewrites the NP background part of the Wilson loop using the nonabelian Stokes theorem [20] as

$$\begin{aligned} \langle W(B) \rangle &= \frac{1}{N_c} \text{tr} \langle P \exp ig \int_C B_\mu dx_\mu \rangle_B = \\ &= \frac{1}{N_c} \text{tr} \langle \exp ig \int_S d\sigma_{\mu\nu} F_{\mu\nu}(u, x_0) \rangle_B. \end{aligned} \quad (25)$$

Here S is a surface bounded by contour C and x_0 – an arbitrary point on S , we also defined:

$$F_{\mu\nu}(u, x_0) = \phi(x_0, u) F_{\mu\nu}(u) \phi(u, x_0) \quad (26)$$

and $\Phi(x, y)$ is the parallel transporter along some contour from y to x .

$$\phi(x, y) = P \exp ig \int_y^x B_\mu(z) dz_\mu \quad (27)$$

To evaluate the last integral in (25) one can use the cluster expansion theorem [21]

$$\langle W(B) \rangle = \frac{1}{N_c} \text{tr exp} \sum_{n=1}^{\infty} \frac{(ig)^n}{n!} \int_S d\sigma(1) \dots \int_S d\sigma(n) \ll F(1) \dots F(n) \gg \quad (28)$$

Here $F(k) \equiv F_{\mu_k \nu_k}(u^{(k)}, x_0)$, $d\sigma(k) \equiv d\sigma_{\mu_k \nu_k}(u^{(k)})$.

The double brackets in (28) denote the cumulant, or connected average, e.g. for $n = 2$

$$\ll F(1)F(2) \gg = \langle F(1)F(2) \rangle - \langle F(1) \rangle \langle F(2) \rangle \quad (29)$$

For more details and definitions of cluster expansion see [21].

Throughout this review we shall consider cumulants or field correlators (FC) $\ll F(1) \dots F(n) \gg$ as the basic NP input, which defines all dynamics of the quark–gluon systems, both for relativistic or nonrelativistic situations and potential or nonpotential regimes. It is a rigorous and explicit language which allows to derive properties of confinement and CSB from the structure of cumulants, as will be shown below. On the other hand, FC are gauge–invariant and Lorentz–covariant quantities which can be found independently, both analytically and on the lattice. Analytic studies of the lowest cumulant $\langle FF \rangle$ have been done recently in [9], using selfcoupled equations which exist for large N_c . Lattice studies are by now numerous for $\langle FF \rangle$ [22–25] and also quartic FC–cumulant $\ll FFFF \gg$ – was studied in [26].

Let us discuss first confinement, i.e. the area law (6) in terms of FC. To this end we rewrite (28) as

$$\langle W(B) \rangle = \frac{1}{N_c} \text{tr exp} \left[-\frac{1}{2} \int_S d\sigma_{\mu\nu}(u) \int_S d\sigma_{\rho\sigma}(v) \Lambda_{\mu\nu, \rho\sigma}(u, v, C) \right] \quad (30)$$

where the global correlator Λ is introduced,

$$\begin{aligned} \Lambda_{\mu\nu, \rho\sigma}(u, v, C) &\equiv g^2 \ll F_{\mu\nu}(u, x_0) F_{\rho\sigma}(v, x_0) \gg - \\ &- 2 \sum_{n=3}^{\infty} \frac{(ig)^n}{n!} \int d\sigma(3) \dots d\sigma(n) \text{perm} \ll F(u) F(v) F(3) \dots F(n) \gg \end{aligned} \quad (31)$$

and *perm* denotes sum over permutations of $F(u)$, $F(v)$ and other terms in the cumulant.

Consider now the lowest term in (31), $\ll FF \gg$.

Both from lattice measurements [22–25] and analytic study [9] this term decays exponentially with $|u - v|$ and the characteristic correlation length T_g , which is called the gluon correlation length, is rather small,

$$T_g = 0.2 \div 0.3 \text{ fm} \quad (32)$$

This quantity is a basic characteristic of the QCD vacuum, defining different dynamical regimes for systems of the range R , in cases $R \langle T_g$ or $R \gg T_g$, as will be shown in chapter 5. For an earlier discussion of T_g see [27].

Consider now Wilson loop of large radius R , $R \gg T_g$. Then in the integral (30) the generic situation is when $|u - x_0|, |v - x_0|$ of the order of R . In this case the correlator $\langle F_{\mu\nu}(u, x_0) F_{\rho\sigma}(v, x_0) \rangle$ does not depend on x_0 (up to the terms $O(T_g^2/R^2)$) and can be rewritten as the function of $|u - v|$. The general decomposition then can written as [28]

$$g^2 \text{tr} \langle F_{\mu\nu}(x_1) \Phi(x_1 x_2) F_{\lambda\sigma}(x_2) \Phi(x_2, x_1) \rangle = N_c [(\delta_{\mu\lambda} \delta_{\nu\sigma} - \delta_{\mu\sigma} \delta_{\nu\lambda}) D(u) + \quad (33)$$

$$+\frac{1}{2}\left(\frac{\partial}{\partial x_{1\mu}}u_\lambda \cdot \delta_{\nu\sigma} + \frac{\partial}{\partial x_{1\lambda}}u_\mu \delta_{\nu\sigma} + perm\right)D_1(u)$$

Insertion of (33) in the integral yields readily the Wilson area law

$$\langle W(B) \rangle = exp(-\sigma S - \gamma P) \quad (34)$$

where σ is expressed through the function $D(x)$, while the perimeter term γP is due to both D and D_1 ,

$$\sigma = \frac{1}{2} \int d^2x D(x) + \dots \quad (35)$$

The ellipsis in (35) implies possible contribution of higher correlators in (31). For all of them, as well as for the Gaussian correlator, a condition necessary to contribute to the string tension σ is that they should contain "Kronecker component", like $D(x)$, which is a coefficient of product of Kronecker δ symbols.

As a consequence this term violates Abelian Bianchi identities [28] (which can be checked acting on both sides of (33) with operators $\varepsilon_{\alpha\beta\mu\nu} \frac{\partial}{\partial x_\beta}$) and hence is connected with the contribution of abelian projected monopoles. This is one of the possible illustration of the physical mechanism of confinement induced by correlator $D(x)$ (and similar higher correlators).

Let us come back to the gluonic correlation length T_g , which together with σ constitute the basic nonperturbative scales. Actually one can calculate T_g through σ , as it was done in [9] using equations for correlators, and through gluon condensate using QCD sum rules [29]. In both cases $T_g \ll \Lambda_{QCD}$ and $T_g \ll \frac{1}{\sqrt{\sigma}}$, which means that T_g signifies a new physical scale. The physical meaning of T_g can be understood, when one calculates the field distribution in the QCD string [26], where Gaussian correlator $D(x)$ yields a very good description of lattice data and reveals that T_g defines the width l of the QCD string (where fields decrease by 50%), namely $l \sim 2T_g$. From lattice data [26] one has

$$l = 0.4 \div 0.5 fm, \quad T_g = 0.2 \div 0.3 fm. \quad (36)$$

In what follows we shall sometimes use the limit $T_g \rightarrow 0$, which we shall call "the string limit". Actually this is the limit of thin strings which is as a rule much simpler than dynamics of the realistic QCD string of finite width (the same limit is always assumed in the theory of strings and superstrings).

The finite value of T_g brings about specific effects. E.g. for the potential of static quarks $V(r)$, which is obtained from the Wilson loop as in (10), one can express $V(r)$ through $D(x)$ and higher correlators, and analyze the large and small- r behaviour, which yields [28]

$$V(r) = \sigma r - c_0, \quad r \rightarrow \infty; \quad V(r) \sim c_2 r^2 + c_4 r^4 + \dots, \quad r \lesssim T_g \quad (37)$$

where $c_0 \sim \sigma T_g$, c_2 is expressed through $D(x)$, c_4 through quartic correlator and so on. Eq.(37) demonstrates that NP fields (B_μ) are soft and yield analytic behaviour of $V(r)$ at $r \ll T_g$, corresponding to the OPE. Interference of perturbative and NP fields may change this picture at small r yielding linear term in r , as was shown in [30]. For more discussion in connection with OPE and QCD sum rules see [31]. We shall not go into details of this phenomenon, but mention that linear behaviour at small r is phenomenologically necessary for good description of fine structure of heavy quarkonia [19,32] and was found recently on the lattice [14].

We end this section with the discussion of the validity of Gaussian approximation, when only quadratic correlator $\langle FF \rangle$ is taken into account. There are arguments in favour of Gaussian approximation both from comparison with lattice data and from the structure of the method.

The first arguments come from the analysis of field distribution inside the string made in [26], as was discussed above. There the largest omitted contribution (from the quartic correlator) amounts to less than few percent. Another comparison is for the static potentials in higher representations, which demonstrate in numerous lattice data [33] (for earlier data see in [1]) a clear Casimir scaling. This is in agreement with the Gaussian approximation, while the quartic term would violate the Casimir scaling [1],[34]. From the numerical accuracy of the latter one can again deduce, that Gaussian approximation is valid within 10% of accuracy, or even better.

Finally one can estimate the parameter of cluster expansion as follows. All observables are expressed in terms of connected FC of gluonic fields, $\langle\langle F(1)...F(n) \rangle\rangle$. E.g. the string tension for heavy (static) quarks is an infinite sum of FC of the field $F_{14} \equiv E_1$ integrated over the plane 14:

$$\sigma \sim \sum_n \frac{g^n}{n!} \prod d^2 r_i \langle\langle E_1(0)E_1(r_1)E_1(r_1+r_2)...E_1(\sum r) \rangle\rangle \quad (38)$$

One can identify parameter of expansion in the sum (38) to be (only even powers of n enter the sum)

$$\zeta = (\bar{E}_1 T_g^2)^2 \quad (39)$$

where T_g is the gluonic correlation length in the vacuum defined by the exponential decay of FC, and $\bar{E}_1^2 \cong g^2 \langle (E_1^a)^2 \rangle = \frac{4\pi^2}{12} G_2 \approx (0.2 GeV)^2$ while G_2 is the standard gluon condensate.

Lattice calculations confirm that T_g is rather small [22-25], indeed $T_g \approx 0.2 \div 0.3 fm$ and therefore ζ is a good expansion parameter

$$\zeta = 0.04 \div 0.1 \quad (40)$$

The regime (40) $\zeta \ll 1$ which seems to be characteristic of real QCD, can be called the regime of the weak confinement. In this case the dynamics of quarks and gluons is adequately described in all known cases by the lowest (Gaussian) correlator.

One should mention the negative feature of Gaussian approximation. Whereas the global correlator $\Lambda_{\mu\nu,\rho\sigma}$ – containing the infinite sum over reduced correlators (cumulants) yields the area law for the Wilson law, not depending on the shape of the surface being integrated in (31), and hence reducing to the minimal surface, retaining only Gaussian correlator one gets as a price for simplification the parasitic dependence on the shape of the surface S in (30). Therefore saying about the dominant role of the Gaussian correlator and smallness of discarded terms one should specify that estimates refer to the minimal surface. On the other hand for an arbitrary surface of any weird shape the contribution of higher correlators can be large and this is what exactly needed for compensation of the extra area contribution of the Gaussian correlator.

The situation here is the same as in the QCD perturbation series, which depends on the normalization mass μ for any finite number of terms of the series. This unphysical dependence is usually treated by fixing μ at some physically reasonable value μ_0 of the order of the inverse size of the system.

In what follows we shall **not** use Gaussian approximation, expert for calculation of spindependent contributions, which amounts to a relatively small correction in good agreement with lattice data and experiment.

4 Background perturbation theory and definition of hadron states

To define the perturbation theory series in ga_μ one starts from (8) and rewrites the Lagrangian as follows:

$$\begin{aligned} L_{tot} &= L_{gf} + L_{gh} + L(B + a) = \\ &L_0 + L_1 + L_2 + L_{int} + L_{gf} + L_{gh} \end{aligned} \quad (41)$$

where L_i have the form:

$$\begin{aligned} L_2(a) &= \frac{1}{2}a_\nu(\hat{D}_\lambda^2\delta_{\mu\nu} - \hat{D}_\mu\hat{D}_\nu + ig\hat{F}_{\mu\nu})a_\mu = \\ &= \frac{1}{2}a_\nu^c[D_\lambda^{ca}D_\lambda^{ad}\delta_{\mu\nu} - D_\mu^{ca}D_\nu^{ad} - g f^{cad}F_{\mu\nu}^a]a_\mu^d, \end{aligned} \quad (42)$$

$$\begin{aligned} D_\lambda^{ca} &= \partial_\lambda \cdot \delta_{ca} + g f^{cba}B_\lambda^b \equiv \hat{D}_\lambda \\ L_0 &= -\frac{1}{4}(F_{\mu\nu}^a(B))^2; \quad L_1 = a_\nu^c D_\mu^{ca}(B)F_{\mu\nu}^a \\ L_{int} &= -\frac{1}{2}(D_\mu(B)a_\nu - D_\nu(B)a_\mu)^a g f^{abc}a_\mu^b a_\nu^c - \frac{1}{4}g^2 f^{abc}a_\mu^b a_\nu^c f^{aef}a_\mu^e a_\nu^f \end{aligned} \quad (43)$$

$$L_{ghost} = -\theta_a^+(D_\mu(B)D_\mu(B+a))_{ab}\theta_b. \quad (44)$$

To calculate Green's functions of any hadrons one can use (8) and write

$$\begin{aligned} G_h(X; Y) &= const \int DB_\mu \eta(B) D\psi D\bar{\psi} Da_\mu \Psi_f^+(X) \Psi_{in}(Y) e^{L_{tot}} \\ &\equiv \langle \Psi_f^+(X) \Psi_{in}(Y) \rangle_{B, \psi, a} \end{aligned} \quad (45)$$

Here $\Psi_{f, in}$ are initial and final hadron states made of $B, \psi, \bar{\psi}, a$. To calculate integral Da_μ one can use perturbative expansion in ga_μ , i.e. neglect in first approximation L_{int} , containing terms a^3, a^4 and take into account only quadratic terms L_2, L_{gf}, L_{gh} . contribution of L_1 was studied in [11] and it was shown there that for the most processes (e.g. for hadron Green's functions) it can be neglected (with accuracy of about better than 10%).

It is convenient to choose background gauge for a_μ , $D_\mu a_\mu = 0$, and take gauge transformation in the form

$$B_\mu \rightarrow U^+(B_\mu + \frac{i}{g}\partial_\mu)U, a_\mu \rightarrow U^+ a_\mu U \quad (46)$$

Now one can choose Ψ_f, Ψ_{in} as gauge-invariant forms built from $B_\mu, a_\mu, \psi, \bar{\psi}$ and to average over $B_\mu, \psi, \bar{\psi}, a_\mu$ as shown in (45). Integrating over DB_μ might seem an impossible adventure due to unknown $\eta(B)$, but we shall see that it can be always written as products of Wilson loops with some insertions, which can be treated in two ways:

i) or in the form of the area law. Then contribution of fields B_μ is given and fixed by the string tension $\sigma(B)$. Equating $\sigma(B) = \sigma_{exper}$ one fixes contribution of the background fields.

ii) Using cluster expansion, and expressing result through lowest correlators, e.g. $\langle FF \rangle$, or $D(x)$ and $D_1(x)$. In this case background is fixed by these functions taken as an input, e.g. from lattice data.

The rest integrals, over $Da_\mu D\psi D\bar{\psi}$ are Gaussian and can be simply done. Now we turn to the construction of $\Psi_{f,in}$.

One can choose local or nonlocal forms for $\Psi_{in,f}$, the latter are obtained by insertion of $\phi(x, y)$ (27) in the local expressions, which are

$$\Psi_{in,f} = \bar{\psi}\Gamma_i\psi \text{ for mesons, } \Gamma_i = 1, \gamma_5, \gamma_\mu, \gamma_\mu\gamma_5, \sigma_{\mu\nu}$$

$$\Psi_{in,f} = \bar{\psi}\Gamma_i f(a, Da)\psi \text{ for hybrids, where } f \text{ is a polynomial, the simplest form is } \bar{\psi}\gamma_i a_\mu\psi$$

$\Psi_{in,f} = \text{tra}\Lambda_2 a$ and $\text{tr}(\Lambda_3 a^3)$ for glueballs made of 2 and 3 gluons respectively. Λ_2, Λ_3 are polynomials made of $D_\mu(B)$ and ensure the needed tensor structure for given quantum numbers. In the simplest case $\Lambda_2 = \Lambda_3 = 1$.

$\Psi_{in,f} = e_{abc}\psi_{f_1\alpha}^a\psi_{f_2\beta}^b\psi_{f_3\gamma}^c K^{f_1\alpha, f_2\beta, f_3\gamma}$ for baryons, where a, f_i, α are color, flavour and Lorentz index respectively.

It is clear that higher hybrid states for mesons and baryons are obtained by adding additional factors of a_μ in $\Psi_{in,f}$.

Several comments are in order. Our definition of hybrids differs from that of the flux tube model [35], where hybrid state is a result of the string excitation. In the latter case the quantum numbers of the hybrid are fixed by the mode of the string. In our case gluon a_μ sitting on the string has its own spin and makes account for larger set of values¹. Also dynamics is different and local state $\Psi_{in,f}$ for hybrid in the flux tube model does not exist. The same differences exist for glueballs. In contrast to other definitions our definition of hybrids and glueballs is unique and is given in the field theoretical terms. The correspondence with the lattice is also clear: to the gluonic excitation in $\Psi_{in,f}$ there corresponds a plaquette on the parallel transporter, which is field strength $F_{\mu\nu}$ in the continuum limit, (or a shift corresponding to an extra link, which is A_μ or D_μ in the continuum).

Insertion of given $\Psi_{in,f}$ in (45) yields after integration over $Da_\mu D\psi D\bar{\psi}$ the hadron Green's function, which can be written [36] respectively for mesons

$$\begin{aligned} G_M(X, Y) &= \langle \text{tr}(\Gamma_i^{(f)}(X)G_q(X, Y)\Gamma_k^{(in)}(Y)G_{\bar{q}}(X, Y)) \rangle_B \\ &\quad - \langle \text{tr}(\Gamma_i^{(f)}(X)G_q(X, X))\text{tr}(\Gamma_k^{(in)}(Y)G_{\bar{q}}(Y, Y)) \rangle_B, \end{aligned} \quad (47)$$

where $G_{q,\bar{q}}$ is the quark (antiquark) Green's function,

$$G_q(X, Y) = (-i\hat{\partial} - im - g\hat{B})_{X,Y}^{-1}, \quad (48)$$

for hybrids

$$G_{hyb}(X, Y) = \langle \text{tr}(\Gamma_i^{(f)}(X)G_q(X, Y)G_g(X, Y)\Gamma_k^{(in)}G_{\bar{q}}(X, Y)) \rangle_B, \quad (49)$$

where G_g is the gluon Green's function(9).

For glueballs one has

$$G_{glueball} = \langle \text{tr}(\Lambda_2^{(f)}(X)G_g(X, Y)\Lambda_2^{(in)}(Y)G_g(X, Y)) \rangle_B \quad (50)$$

and for baryons

$$G_B(X, Y) = \langle \text{tr}(eK^{(f)} \prod_{i=1}^3 G_q^{(i)}(X, Y)eK^{(in)}) \rangle_B \quad (51)$$

¹the author is grateful to Yu.Kalashnikova for a discussion of this point

The structure of hadron Green's function is clear: it is a product of quark and gluon Green's function averaged over the background field B_μ . In the next section we shall discuss the way, how to make this averaging explicit and express it through the Wilson loop.

So far we have neglected interaction of propagating quarks and gluons with the perturbative field a_μ , i.e. color Coulomb exchanges. For quarks those can be easily restored and summed up in the exponent [37,38] as we shall show below; for propagating gluons perturbative exchanges do not reduce to color Coulomb interaction, and should be treated perturbatively term by term [39]. It was discussed in [39] that next-to-leading corrections strongly damp the main term.

5 Relativistic path integrals and relativistic Hamiltonians

In this section we shall discuss relativistic path integrals in the form of Feynman–Schwinger representation (FSR), first introduced for hadron Green's functions in [36] and later developed in [37], (for earlier references to FSR see [36–38] and [42]) and relativistic Hamiltonians which were obtained from FSR in [4,5]. These Hamiltonians will be used in the next sections to calculate relativistic spectrum of mesons and baryons, and also hybrids and glueballs.

The basic approximation which will be used in this section is the perturbative treatment of spin degrees of freedom, i.e. of fine and hyperfine spin interactions. As one will see, for most mesons and baryons (except for Nambu–Goldstone mesons π and K) this is a good approximation and the resulting spectra are in good agreement with experiment.

A more general treatment, valid also for Nambu–Goldstone mesons and displaying chiral symmetry breaking, will be discussed in the second part of these lectures.

We start with the meson Green's function (47) and for simplicity consider flavour nonsinglet meson, so the last term on the r.h.s. of (47) is absent.

For the quark Green's function in the external field $A_\mu = B_\mu + a_\mu$ one can write the FSR [36,37]

$$G_q(x, y) = (m - \hat{D}) \int_0^\infty ds (Dz)_{xy} e^{-K} \Phi_\sigma(x, y) \quad (52)$$

where notations used are

$$K = m^2 s + \frac{1}{4} \int_0^s d\tau \left(\frac{dz_\mu}{d\tau} \right)^2; \quad D_\mu = \partial_\mu - ig A_\mu, \quad (53)$$

$$(Dz)_{xy} = \lim_{N \rightarrow \infty} \prod_{n=1}^N \frac{d^4 \xi(n)}{(4\pi\varepsilon)^2} \frac{d^4 q}{(2\pi)^4} e^{iq(\sum \xi(n) - (x-y))}, \quad N\varepsilon = s \quad (54)$$

$$\Phi_\sigma(x, y) = P_A P_F \exp(ig \int_y^x A_\mu dz_\mu) \exp(g \int_0^s d\tau \sigma_{\mu\nu} F_{\mu\nu}), \quad (55)$$

and

$$\sigma_{\mu\nu} = \frac{1}{4i} (\gamma_\mu \gamma_\nu - \gamma_\nu \gamma_\mu), \quad \xi(n) = z(n) - z(n-1).$$

One can write the same FSR for the antiquark Green's function; taking into account that in this case one should use the charge-conjugated field

$$A_\mu^{(C)} = C^{-1} A_\mu C = -A_\mu^T, \quad F_{\mu\nu}^{(C)} = -F_{\mu\nu}^T \quad (56)$$

the ordering of $P_A P_F$ in (55) changes its direction as well as limits of integration $(x, y) \rightarrow (y, x)$. As a result one obtains the meson Green's function as the path integral over closed Wilson loops with insertion of magnetic moment terms $\sigma_{\mu\nu} F_{\mu\nu}$ of different signs for quark and antiquark, as it should be,

$$G_M(x, y) = \langle \text{tr} \Gamma^{(f)}(m - \hat{D}) \int_0^\infty ds \int_0^\infty d\bar{s} e^{-K - \bar{K}} (Dz)_{xy} (D\bar{z})_{xy} \Gamma^{(i)}(\bar{m} - \hat{\bar{D}}) W_F \rangle \quad (57)$$

Here the bar sign refers to the antiquark, and

$$W_F = P_A P_F \exp(ig \oint dz_\mu A_\mu) \exp(g \int_0^s d\tau \sigma_{\mu\nu}^{(1)} F_{\mu\nu}) \exp(-g \int_0^{\bar{s}} \sigma_{\mu\nu}^{(2)} F_{\mu\nu} d\bar{\tau}) \quad (58)$$

In (57) enter integrations over proper times s, \bar{s} and $\tau, \bar{\tau}$, which also play the role of ordering parameter along the trajectory, $z_\mu = z_\mu(\tau)$, $\bar{z}_\mu = \bar{z}_\mu(\bar{\tau})$.

It is convenient to go over to the actual time $t \equiv z_4$ of the quark (or antiquark), defining the new quantity $\mu(t)$, which will play very important role in what follows

$$2\mu(t) = \frac{dt}{d\tau}, \quad t \equiv z_4(\tau) \quad (59)$$

For each quark (or antiquark and gluon) one can rewrite the path integral (52), (57) as follows (see appendix 1 of the second paper in [5] for details of derivation)

$$\int_0^\infty ds (D^4 z)_{xy} \dots = \text{const} \int D\mu(t) (D^3 z)_{xy} \dots \quad (60)$$

where $(D^3 z)_{xy}$ has the same form as in (54) but with all 4-vectors replaced by 3-vectors, and the path integral $D\mu(t)$ is supplied with the proper integration measure, which is derived from the free motion Lagrangian.

In general $\mu(t)$ can be a strongly oscillating function of t due to the Zitterbewegung. In what follows we shall use the steepest descent method for the evaluation of the integral over $D\mu(t)$, with the extremal $\mu_0(t)$ playing the role of effective or constituent quark mass. We shall see that in all cases, where spin terms can be considered as a small perturbation, i.e. for majority of mesons, μ_0 is positive and rather large even for vanishing quark current masses m, \bar{m} , and the role of Zitterbewegung is small (less than 10% from the comparison to the light-cone Hamiltonian eigenvalues, see [40,41] for details).

Now the kinetic terms can be rewritten using (59) as

$$K + \bar{K} = \int_0^T dt \left\{ \frac{m^2}{2\mu(t)} + \frac{\mu(t)}{2} [(\dot{z}_i(t))^2 + 1] + \frac{\bar{m}^2}{2\bar{\mu}(t)} + \frac{\bar{\mu}(t)}{2} [(\dot{\bar{z}}_i(t))^2 + 1] \right\} \quad (61)$$

where $T = x_4 - y_4$. In the spin-dependent factors the corresponding changes are

$$\int_0^s d\tau \sigma_{\mu\nu} F_{\mu\nu} = \int_0^T \frac{dt}{2\mu(t)} \sigma_{\mu\nu} F_{\mu\nu}(z(t)). \quad (62)$$

In what follows in this section we shall systematically do perturbation expansion of the spin terms, since otherwise (57) cannot be estimated. Therefore as the starting approximation we shall use the Green's functions of mesons made of spinless quarks, which amounts to neglect in (57),(58) terms $(m - \hat{D})$, $(\bar{m} - \hat{\bar{D}})$ and $\sigma_{\mu\nu} F_{\mu\nu}$. As a result one has

$$G_M^{(0)}(x, y) = \text{const} \int D\mu(t) D\bar{\mu}(t) (D^3 z)_{xy} (D^3 \bar{z})_{xy} e^{-K - \bar{K}} \langle W \rangle. \quad (63)$$

Our next approximation is the neglect of perturbative exchanges in $\langle W \rangle$, which yields for large Wilson loops, $R, T \gg T_g$,

$$\langle W \rangle_B = \text{const} \exp(-\sigma S_{min}) \quad (64)$$

where S_{min} is the minimal area inside the given trajectories of quark and antiquark,

$$S_{min} = \int_0^T dt \int_0^1 d\beta \sqrt{\det g}, \quad g_{ab} = \partial_a w_\mu \partial_b w^\mu, \quad a, b = t, \beta. \quad (65)$$

The Nambu-Goto form of S_{min} cannot be quantized due to the square root and one has to use the auxiliary field approach [42] with functions $\nu(\beta, t)$ and $\eta(\beta, t)$ to get rid of the square root, as it is usual in string theories. As the result the total Euclidean action becomes [5]

$$\begin{aligned} A = K + \bar{K} + \sigma S_{min} = & \int_0^T dt \int_0^1 d\beta \left\{ \frac{1}{2} \left(\frac{m^2}{\mu(t)} + \frac{\bar{m}^2}{\bar{\mu}(t)} \right) + \frac{\mu_+(t)}{2} \dot{R}^2 + \right. \\ & \left. + \frac{\tilde{\mu}(t)}{2} \dot{r}^2 + \frac{\nu}{2} [\dot{w}^2 + \left(\frac{\sigma}{\nu} \right)^2 r^2 - 2\eta(\dot{w}r) + \eta^2 r^2] \right\}. \end{aligned} \quad (66)$$

Here $\mu_+ = \mu + \bar{\mu}$, $\tilde{\mu} = \frac{\mu\bar{\mu}}{\mu+\bar{\mu}}$, $R_i = \frac{\mu z_i + \bar{\mu} \bar{z}_i}{\mu + \bar{\mu}}$, $r_i = z_i - \bar{z}_i$. Note, that integrations over μ, ν and η effectively amount to the replacement by their extremum values [5].

Performing Gaussian integrations over R_μ and η one arrives in the standard way at the Hamiltonian (we take $m = \bar{m}$ for simplicity)

$$\begin{aligned} H = & \frac{p_r^2 + m^2}{\mu(\tau)} + \mu(\tau) + \frac{\hat{L}^2/r^2}{\mu + 2 \int_0^1 (\beta - \frac{1}{2})^2 \nu(\beta) d\beta} + \\ & + \frac{\sigma^2 r^2}{2} \int_0^1 \frac{d\beta}{\nu(\beta)} + \int_0^1 \frac{\nu(\beta)}{2} d\beta, \end{aligned} \quad (67)$$

where $p_r^2 = (\mathbf{p}\mathbf{r})^2/r^2$, and L is the angular momentum, $\hat{L} = (\mathbf{r} \times \mathbf{p})$.

The physical meaning of the terms $\mu(t)$ and $\nu(\beta)$ can be understood when one finds their extremal values. E.g. when $\sigma = 0$ and $L = 0$, one finds from (67)

$$H_0 = 2\sqrt{\mathbf{p}^2 + m^2}, \quad \mu_0 = \sqrt{\mathbf{p}^2 + m^2} \quad (68)$$

so that μ_0 is the energy of the quark. Similarly in the limiting case $L \rightarrow \infty$ the extremum over $\nu(\beta)$ yields:

$$\nu_0(\beta) = \frac{\sigma r}{\sqrt{1 - 4y^2(\beta - \frac{1}{2})^2}}, \quad H_0^2 = 2\pi\sigma\sqrt{L(L+1)} \quad (69)$$

so that ν_0 is the energy density along the string with the β playing the role of the coordinate along the string.

Let us start with the $L = 0$ case. Taking extremum in $\nu(\beta)$ one has

$$H_1 = \frac{p_r^2 + m^2}{\mu(t)} + \mu(t) + \sigma r. \quad (70)$$

Here $\mu(t)$ is to be found also from the extremum and is therefore an operator in Hamiltonian formalism. Taking extremum in $\mu(t)$ one obtains

$$H_2 = 2\sqrt{p_r^2 + m^2} + \sigma r. \quad (71)$$

The Hamiltonian (71) is what one traditionally exploits in the relativistic quark model (RQM) [6-8] (apart from color Coulomb and spin-dependent terms to be discussed below). The RQM was an essential step in our understanding of hadronic spectra, see especially [7] for an encyclopedic survey of model predictions. At the same time the usual input of RQM contains too many parameters and the model was introduced rather ad hoc. Another deficiency of this model at this point is twofold:

i) one usually takes m in (71) to be constituent quark mass of the order of 100-200 MeV, which is introduced as an input. Instead we have in (71) the current quark mass renormalized at the reasonable scale of 1 GeV. Hence it is almost zero for light quarks;

ii) the form (71) is used in RQM for any L , and to this end one writes in (71) $p_r^2 \rightarrow \mathbf{p}^2$.

However the Regge slope for both (70) and (71) is $1/8\sigma$ instead of the string slope $\frac{1}{2\pi\sigma}$, which occurs for the total Hamiltonian (69), since the RQM Hamiltonian (71) does not take into account string rotation.

Still for $L = 0$ the form (71) is a good starting approximation, and it is rewarding that our systematic approach makes here contact with RQM. Sometimes it is convenient to use instead of (71) a more tractable form (70) where $\mu(t) = \mu_0$ and μ_0 is to be found from the extremum of the eigenvalue of Hamiltonian H_1 :

$$H_1\psi = M_1\psi, \quad M_1 = M_1(\mu_0), \quad \frac{\partial M_1}{\partial \mu_0} = 0. \quad (72)$$

This procedure was suggested in [4], and its accuracy was tested recently in [43]. In Table 1 listed are eigenvalues of (72) and (71) ($M_n^{(1)}$ and $M_n^{(2)}$ respectively) for several values of the radial quantum number n .

One can see that the difference between $M_n^{(1)}$ and $M_n^{(2)}$ is around 5%.

Equation (70), (72) can be reduced to the Airy equation with the eigenvalues written as (for $m = 0$)

$$M_n^{(1)} = 4\mu_0(n), \quad \mu_0(n) = \sqrt{\sigma} \left(\frac{a(n)}{3} \right)^{3/4} \quad (73)$$

where $a(n)$ is the corresponding zero of the Airy function. The Table 2 gives a set of lowest $a(n)$ and $\mu_0(n)$ for $L = 0, 1, 2$. The $\mu_0(n)$ for nonzero L values, $L = 1, 2$ are used later for spin splittings of obtained levels. The first comprehensive study of the equation (70) with fixed $\mu(t) \equiv m$ was done in [44], where also $a(n)$ are quoted (called there $\zeta(n, L)$).

Finally we turn to the Hamiltonian (67), where the eigenvalues have been found in [43] using WKB method. The corresponding values are listed in Table 3 for the case $m = 0$.

An equivalent numerical method was used to find eigenvalues of the rotating string with quarks at the ends in [45], which should be compared with the entries of Table 3 and agree with accuracy of about 5%. Comparing mass eigenvalues in Table 1-3 one can notice that they are too heavy to reproduce the experimental values, and one needs to subtract some 700-800 MeV to get to the region of ρ -meson. In RQM one introduces by hand a large negative constant in the Hamiltonian, subtracting just this amount. In our approach here when spins are treated as a perturbation we do not understand how this large negative constant occurs. Indeed, there appears a constant c_0 due to the finite string width, but this is too small $c_0 \approx 0.1 \div 0.2$ GeV to explain the effect. It is clear however, that this constant is due to nonperturbative selfenergies of the quark and antiquark, and should be sensitive to the quark current mass (i.e. flavour) and chiral symmetry breaking. As we shall show in the second part of these lectures (to be published separately), the solution of this problem, which may be called" the Regge intercept

problem”, lies in the correct treatment of spin and chiral degrees of freedom, and to obtain a correct Regge intercept of meson trajectory one should go beyond the perturbation theory for spin effects.

Generalization of (67) to the case of unequal current masses of quarks is straightforward [60]

$$H = \frac{m^2}{2\mu} + \frac{\bar{m}^2}{2\bar{\mu}} + \frac{\mu_+}{2} + \frac{p_r^2}{2\tilde{\mu}} + \frac{\hat{L}^2/r^2}{2(\mu_1(1-\zeta)^2 + \mu_2\zeta^2 + \int_0^1 d\beta(\beta-\zeta)^2\nu(\beta))} + \frac{\sigma^2 r^2}{2} \int_0^1 \frac{d\beta}{\nu(\beta)} + \int_0^1 \frac{\nu(\beta)}{2} d\beta, \quad (74)$$

where we have defined $\zeta = \frac{\mu_+ \int \beta \nu d\beta}{\mu_+ \bar{\mu}_+ \int \nu d\beta}$.

For $L = 0$ one can as before find extremum in $\nu(\beta)$ and obtain Hamiltonian

$$H^1 = \frac{m^2}{2\mu} + \frac{\bar{m}^2}{2\bar{\mu}} + \frac{\mu_+}{2} + \frac{p_r^2}{2\bar{\mu}} + \sigma r \quad (75)$$

A simplified procedure of solving (75) as in the case of equal mass, (72), reduces to the solution of Schroedinger-like equation and to the finding $\mu, \bar{\mu}$ from the extremum of the total mass [46],

$$H^1 \Psi = M(\mu, \bar{\mu}) \Psi, \quad \bar{M} = M(\mu_0, \bar{\mu}),$$

$$\frac{\partial M}{\partial \mu_0} = \frac{\partial M}{\partial \bar{\mu}_0} = 0 \quad (76)$$

here $M(\mu, \bar{\mu})$ can be expressed through the same standard numbers $a(n)$ as given in (73) and Table 2, namely

$$M(\mu, \bar{\mu}) = \frac{m^2}{2\mu} + \frac{\bar{m}^2}{2\bar{\mu}} + \frac{\mu_+}{2} + \varepsilon_n(\tilde{\mu}), \quad \varepsilon_n(\tilde{\mu}) = (2\tilde{\mu})^{-1/3} \sigma^{2/3} a(n). \quad (77)$$

Extremum conditions for μ and $\bar{\mu}$ look like

$$-\frac{m^2}{2\mu^2} + \frac{1}{2} - \frac{\sigma^{2/3} a(n) \mu^{-4/3} \bar{\mu}^{2/3}}{2^{1/3} 3 (\mu + \bar{\mu})^{2/3}} = 0 \quad (78)$$

$$-\frac{\bar{m}^2}{2\bar{\mu}^2} + \frac{1}{2} - \frac{\sigma^{2/3} a(n) \bar{\mu}^{-4/3} \mu^{2/3}}{2^{1/3} 3 (\mu + \bar{\mu})^{2/3}} = 0 \quad (79)$$

From (78), (79) one can see that whenever the current mass is large, $m \ll \sqrt{\sigma}$, the constituent mass is close to the current mass, indeed first terms of expansion are

$$\mu^2 \cong m^2 \left[1 + \frac{a(n)}{3} \left(\frac{2\sigma\bar{\mu}}{m^2(m+\bar{\mu})} \right)^{2/3} \right] \quad (80)$$

Till now perturbative gluon exchanges and spin dependent terms in Green's functions and Hamiltonians have been neglected. Now we are going to restore their contribution and consider to this end the general form (57).

Leaving out for the moment spin terms $\sigma_{\mu\nu}F_{\mu\nu}$, we have to do with the Wilson loop containing both perturbative and NP fields, $W(B+a)$. For the purely perturbative interaction, one can use theorem of cluster expansion to get

$$\frac{1}{N_c} \langle \text{tr} W(a) \rangle = \exp\left[-\frac{g^2}{2} \int \int dz_\mu dz'_\nu \langle \langle a_\mu(z) a_\nu(z') \rangle \rangle\right] + O(g^4) \quad (81)$$

Introducing perturbative Green's function (in the Feynman gauge for simplicity)

$$\langle \langle a_\mu(z) a_\nu(z') \rangle \rangle = \frac{\delta_{\mu\nu}}{(2\pi)^2} (z-z')^{-2} \quad (82)$$

and integrating out $z'_4 - z_4$ in $dz_4 dz'_4 = dz_4 d(z'_4 - z_4)$, one obtains the color Coulomb interaction in the exponent

$$\frac{1}{N_c} \langle \text{tr} W(a) \rangle = \exp\left[C_2 \alpha_s \int \frac{dz_4}{|\mathbf{z} - \mathbf{z}'|} + O_1(\alpha_s) + O_2(\alpha_s^2)\right] \quad (83)$$

where $O_1(\alpha_s)$ is the radiative correction coming from the spacial integral $d\mathbf{z}d\mathbf{z}'$ in (81), and $O_2(\alpha_s^2)$ is the corrections coming from quartic and higher correlators of the form

$$\int \int \dots \int \langle \langle a(1)a(2)a(3)\dots a(n) \rangle \rangle dz(1)\dots dz(n), n \geq 4.$$

Coming now to the original Wilson loop, $W(B+a)$, let us write it in the form

$$\frac{1}{N_c} \text{tr} \langle W(B+a) \rangle_{B,a} = \frac{1}{N_c} \text{tr} \langle [W(B)W(a)W_{int}(B,a)] \rangle_{B,a} \quad (84)$$

where $W_{int}(B,a)$ is the interference term, involving both fields B_μ and a_μ . Part of this interference was taken into account in the previous chapter, when the freezing of α_s was considered. This shows that interference may change behaviour of perturbative terms at large distances. Another example of interference was considered recently in [30,31] when treating the small distance behaviour of static potential. In both cases it is seen that the main domain of perturbative fields a_μ is small distance domain, while that of NP fields B_μ is the large distance domain. From the static $Q\bar{Q}$ potential one can deduce that both regions join smoothly at $r_c \approx 0.25 fm$ and perturbative force is strong for $r < r_c$ (and stronger than both NP and interference), while NP force is strong for $r > r_c$ and much stronger than both Coulomb force and interference. So our simplifying assumption is that one can disregard interference term W_{int} altogether, and take it later as a correction.

As a result confining term from $W(B)$ and color Coulomb term enter as a sum, hence it is legitimate to take color Coulomb term as an additional term to be added to the Hamiltonian (74) or (75). Note that this is true both for heavy quarks (nonrelativistic situation) and light quarks (relativistic situation). What is still left over, apart from interference, is radiative corrections $O(\alpha_s)$ and all higher terms in $O(\alpha_s^2)$. The reason why the Coulomb term is retained in (83) as compared to those suppressed, is that Coulomb term is enhanced as $O(1/v)$ for slow quarks and the quadratic term in (81) generates Sudakov-type asymptotics [38].

As was mentioned above, color Coulomb interaction for the $q\bar{q}$ system (situation will be different for gluon systems, see below) is exponentiated in (83) which implies that Coulomb term can be taken to all orders, i.e. one should consider the Hamiltonian

$$H_c = H' - \frac{4}{3} \frac{\alpha_s(r)}{r} \quad (85)$$

where H' is the string Hamiltonian (74) or (75).

One can express the eigenvalue $\varepsilon_n(\tilde{\mu})$ of the H_c through the eigenvalue of the reduced equation, as was done before without Coulomb in (73).

$$\varepsilon_n(\tilde{\mu}) = (2\tilde{\mu})^{-1/3} \sigma^{2/3} a(\lambda, L, n) \quad (86)$$

and the reduced equation looks like [45, 46]

$$\left(-\frac{d^2}{d\rho^2} + |\rho| - \frac{\lambda}{|\rho|}\right)\chi(\rho) = a(\lambda, L, n)\chi(\rho) \quad (87)$$

where

$$\lambda = \frac{4\alpha_s (2\tilde{\mu})^{2/3}}{3 \sigma^{1/3}}, \quad r = \frac{\rho}{(2\tilde{\mu})^{1/3}}, \quad a(\lambda = 0, L, n) = a(L, n). \quad (88)$$

The eigenvalues $a(\lambda, L, n)$ are given in Table 4 for $L = n = 0$.

Finding as before μ and $\bar{\mu}$ from the extremum condition on M_n ,

$$M_n = \frac{m^2}{2\mu} + \frac{\mu}{2} + \frac{\bar{m}^2}{2\mu^2} + \frac{\bar{\mu}}{2} + \varepsilon_n(\tilde{\mu}), \quad (89)$$

one obtains equations [46]

$$1 = \frac{m^2}{\mu^2} + \frac{(2\tilde{\mu})^{2/3} \sigma^{2/3}}{3\mu^2} (a(\lambda) + \left|\frac{\partial a}{\partial \lambda}\right| 2\lambda) \quad (90)$$

$$1 = \frac{\bar{m}^2}{\bar{\mu}^2} + \frac{(2\tilde{\mu})^{2/3} \sigma^{2/3}}{3\bar{\mu}^2} (a(\lambda) + \left|\frac{\partial a}{\partial \lambda}\right| 2\lambda) \quad (91)$$

one should note, that Coulomb attraction strongly affects the values of $\mu, \bar{\mu}$ and wave function at origin.

Connection between eigenfunction $\varphi_n(r)$ of the Hamiltonian (85) and eigenfunction $\chi_n(\rho)$ of the reduced equation (87) is

$$\varphi_n(\mathbf{r}) = (2\tilde{\mu}\sigma)^{\frac{L}{3} + \frac{1}{2}} \chi_n(\rho) Y_{Lm}(\theta, \varphi). \quad (92)$$

For purely linear potential, i.e. for $\lambda = 0$, the value of the function $\varphi_n(0)$ does not depend on n [45,47]

$$|\varphi_n^{(\lambda=0)}(0)|^2 = \frac{2\tilde{\mu}\sigma}{4\pi}, \quad \chi_n^{(\lambda=0)}(0) = 1. \quad (93)$$

Taking into Coulomb potential, i.e. $\lambda \neq 0$; one gets an enhanced value of $\chi_n(0)$, which is given in Table 4. Using these entries and (92) one can calculate $|\varphi_n(0)|^2$ for any $q\bar{q}$ system, which will be used in the next chapter for the hyperfine interaction and for the quark decay constants.

For this quantity the asymptotic freedom is also important and should be taken into account.

The coefficient $\rho(AF) = \left|\frac{\chi^{as}(0)}{\chi(0)}\right|^2$, where $\chi^{as}(\rho)$ is the solution of (87) with $\alpha_s(r)$ in λ decreasing according to asymptotic freedom from the maximal value $\alpha_s^{(0)}$, with $\Lambda_{QCD} = 140 MeV$ is given in Table 5.

Now we turn to the spin terms, considering them as perturbation (a complete treatment of spin terms within new formalism will be given in the last section) In the derivation of spin-dependent interaction valid also for massless quarks the advantage of the present method will

be evident, since the usual treatment exploits expansion in inverse powers of quark masses, appropriate for heavy quarkonia only. In our case the problem reduces to the calculation of averages in (57), (58), with the use of (62). This can be written as [48,49]

$$\langle W_F \rangle = P_F \exp\left(\int_0^T \frac{dt}{2\mu(t)} \sigma_{\mu\nu}^{(1)} \frac{\delta}{i\delta s_{\mu\nu}(z(t))}\right) \exp\left(-\int_0^T \frac{d\bar{t}}{2\bar{\mu}(\bar{t})} \sigma_{\mu\nu}^{(2)} \frac{\delta}{i\delta s_{\mu\nu}(\bar{z}(\bar{t}))}\right) \langle W \rangle \quad (94)$$

where for $\langle W \rangle$ one can use the cluster expansion (28).

In the Gaussian approximation one has ($P_F \rightarrow P_\sigma$)

$$\langle W_F \rangle = P_\sigma \exp(K_1 + K_2 + K_{11} + K_{22} + K_{12}) \langle W \rangle \quad (95)$$

and e.g.

$$K_1 = ig^2 \int_0^T \frac{dt}{2\mu(t)} \sigma_{\mu\nu}^{(1)} \int ds_{\lambda\rho}^{(w)} \langle F_{\mu\nu}(z(t)) F_{\lambda\rho}(w) \rangle, \quad (96)$$

$$K_{12} = -g^2 \int_0^T \frac{dt}{2\mu(t)} \int_0^T \frac{d\bar{t}}{2\bar{\mu}(\bar{t})} \sigma_{\mu\nu}^{(1)} \sigma_{\lambda\rho}^{(2)} \langle F_{\mu\nu}(z(t)) F_{\lambda\rho}(\bar{z}(\bar{t})) \rangle, \quad (97)$$

while other terms are obtained by replacing $\sigma_{\mu\nu}^{(1)} \frac{dt}{2\mu(t)}$ by $\sigma_{\mu\nu}^{(2)} \frac{d\bar{t}}{2\bar{\mu}(\bar{t})}$ or vice versa. In what follows we do not need the selfenergy terms $K_{11}, K_{22} \sim (\sigma_{\mu\nu}^{(i)})^2$.

Now one use representation (33) to express field correlators through $D(u), D_1(u)$. To define the minimal surface for integration in $\langle W \rangle, \langle W_F \rangle$ one connects trajectories of quark $z(t)$ and antiquark $\bar{z}(\bar{t})$ by a smooth line $w(t, \beta)$ at $t = \bar{t}, 0 \leq \beta \leq 1$. One can approximate it by a straight line for simplicity: $w(t, \beta) = z(t)\beta + \bar{z}(\bar{t})(1 - \beta)$.

Introducing angular momenta in Minkowski space

$$L_i^{(1)} = (\mathbf{r} \times \mathbf{p}_1)_i = ie_{ikm} r_k(t) \mu \dot{z}_m(t), \quad (98)$$

$$L_i^{(2)} = (\mathbf{r} \times \mathbf{p}_2)_i = ie_{ikm} r_k(t) \bar{\mu} \dot{\bar{z}}_m(t), \quad (99)$$

one has

$$ds_{ik} = (dw_i \dot{w}_k - dw_k \dot{w}_i) = \frac{1}{i} d\beta dt e_{ikm} \left(\frac{\beta L_m^{(1)}}{\mu} + \frac{(-\beta) L_m^{(2)}}{\bar{\mu}} \right) \quad (100)$$

We refer the reader for details to [48-50].

The resulting spin terms can be written in the Eichten–Feinberg notations [51], namely

$$\begin{aligned} V_{SD}(r) = & \left(\frac{\sigma_i^{(1)} L_i^{(1)}}{4\mu^2} - \frac{\sigma_i^{(2)} L_i^{(2)}}{4\bar{\mu}^2} \right) \left(\frac{1}{r} \frac{d\varepsilon}{dr} + \frac{2}{r} \frac{dV_1}{dr} \right) + \\ & \frac{\sigma_i^{(1)} L_i^{(1)} - \sigma_i^{(2)} L_i^{(2)}}{2\mu\bar{\mu}} \frac{1}{r} \frac{dV_2}{dr} + \frac{\sigma_i^{(1)} \sigma_i^{(2)}}{12\mu\bar{\mu}} V_4(r) + \\ & \frac{1}{12\mu\bar{\mu}} (3\sigma_i^{(1)} n_i \sigma_k^{(2)} n_k - \sigma_i^{(1)} \sigma_i^{(2)}) V_3(r) \end{aligned} \quad (101)$$

and $V_i(r), i = 0, 1, 2, 3, 4$ are expressed through D, D_1 [48,50] as follows.

$$\frac{1}{r} \frac{dV_1}{dr} = - \int_{-\infty}^{\infty} d\nu \int_0^r \frac{d\lambda}{r} \left(1 - \frac{\lambda}{r} \right) D(\lambda, \nu) \quad (102)$$

$$\frac{1}{r} \frac{dV_2}{dr} = \int_{-\infty}^{\infty} d\nu \int_0^r \frac{\lambda d\lambda}{r^2} [D(\lambda, \nu) + D_1(\lambda, \nu) + \lambda^2 \frac{\partial D_1}{\partial \lambda^2}] \quad (103)$$

$$V_3 = - \int_{-\infty}^{\infty} d\nu r^2 \frac{\partial D_1(r, \nu)}{\partial r^2} \quad (104)$$

$$V_4 = \int_{-\infty}^{\infty} d\nu (3D(r, \nu) + 3D_1(r, \nu) + 2r^2 \frac{\partial D_1}{\partial r^2}) \quad (105)$$

$$\frac{1}{r} \frac{d\varepsilon(r)}{dr} = \int_{-\infty}^{\infty} d\nu \int_0^r \frac{d\lambda}{r} [D(\lambda, \nu) + D_1(\lambda, \nu) + (\lambda^2 + \nu^2) \frac{\partial D_1}{\partial \nu^2}] \quad (106)$$

Equations (93-97) give the NP spin-dependent interaction through functions D, D_1 ; the latter have been measured on the lattice [22 - 24] to be of the form

$$D(x) = D(0) \exp\left(-\frac{|x|}{T_g}\right), \quad D_1(x) = D_1(0) \exp\left(-\frac{|x|}{T_g}\right) \quad (107)$$

with $\frac{D_1(0)}{D(0)} = \frac{1}{3}(\frac{1}{7})$, and $T_g = 0.2(0.33)fm$ for quenched [22,23] (dynamical [24]) quarks; while $D(0) = 0.073GeV^4$ for quenched case [22].

Insertion of (107) into (102-106) yields an estimate of all 5 potentials $\varepsilon(r), V_i(r), i = 1, 2, \dots, 4$. The first, $\varepsilon(r)$ is just scalar potential $V(r)$ appearing in (37), and present in (75) in the form σr ; $V_3(r)$ and $V_4(r)$ are numerically small as compared to the perturbative contributions to be discussed below. The largest contribution comes from the spin-orbit term; V_{so} ; since $V_1'(r)|_{r \rightarrow \infty} = -\varepsilon'(r)|_{r \rightarrow \infty} = -\sigma$, one obtains for the equal mass case the asymptotics ($L_i^{(1)} = -L_i^{(2)} = L_i$)

$$V_{so}(r) = -\frac{\sigma \mathbf{S} \mathbf{L}}{2\mu r} f(r), \quad f(r \rightarrow \infty) = 1. \quad (108)$$

For small r the behaviour of $f(r)$ is changed, $f(0) = 0$, and $V_{so}(r \rightarrow 0) = const$. For more details and discussion of the behaviour of $v_i(r)$ and comparison with lattice data see [50].

Analysis of spectra of heavy quarkonia made in [32] strongly prefer $f(0) = 1$, in contradiction with (101-103). The way out may be seen in the interference terms at small r , studied in [30,31], which show that linear dependence of $\varepsilon(r)$ in r may persist at very small r in agreement with a recent dedicated lattice analysis [14].

We turn now to the perturbative contribution to spin-dependent interaction and to this end one can use again the general expressions (101-106) where instead of D, D_1 one should insert the corresponding perturbative expressions. To the order $O(g^2)$ one has

$$D(x) = 0, \quad D_1(x) = \frac{16\alpha_s}{3\pi x^4} \quad (109)$$

Insertion of (109) into (101-106) yields

$$V_{1p} = 0; \quad \frac{1}{R} V_{2p}'(r) = \frac{4\alpha_s}{3R^3}, \quad V_{3p} = \frac{4\alpha_s}{R^3}, \quad \varepsilon_p(R) = -\frac{4\alpha_s}{3R}, \quad V_{4p}(R) = \frac{32\pi\alpha_s}{3} \delta^3(\mathbf{R}). \quad (110)$$

The final expression for the mass of the meson with spin interaction taken into account perturbatively is obtained from (75) and (85), (101) and has the form

$$M_n = \bar{M}_n(\mu_0, \bar{\mu}_0) + \frac{32\mathbf{s}_1 \mathbf{s}_2 \pi \alpha_s}{9\mu_0 \bar{\mu}_0} \varphi_n^2(0) +$$

$$\begin{aligned}
& \left(\frac{\mathbf{s}_1}{2\mu_0^2} + \frac{\mathbf{s}_2}{2\bar{\mu}_0^2}\right)\mathbf{L}\left\langle\frac{-\sigma f(r)}{r}\right\rangle + \left(\frac{\mathbf{S}}{\mu_0\bar{\mu}_0} + \frac{\mathbf{s}_1}{2\bar{\mu}_0^2} + \frac{\mathbf{s}_2}{2\mu_0^2}\right)\mathbf{L}\frac{4}{3}\left\langle\frac{\alpha_s}{r^3}\right\rangle + \\
& \frac{\langle 3\mathbf{s}_1\mathbf{n}\mathbf{s}_2\mathbf{n} - \mathbf{s}_1\mathbf{s}_2 \rangle}{\mu_0\bar{\mu}_0}\frac{4}{3}\left\langle\frac{\alpha_s}{r^3}\right\rangle
\end{aligned} \tag{111}$$

Where $\mathbf{S} = \mathbf{s}_1 + \mathbf{s}_2$, and

$$\bar{M}_n(\mu_0, \bar{\mu}_0) = \frac{m^2}{2\mu_0} + \frac{\mu_0}{2} + \frac{\bar{m}^2}{2\bar{\mu}_0} + \frac{\bar{\mu}_0}{2} + \varepsilon(\bar{\mu}_0) + \Delta M - C_0 \equiv M_n^{(0)} + \Delta M - C_0 \tag{112}$$

Here ΔM takes into account the so-called string correction, i.e. the difference of eigenvalues of the Hamiltonian (67) and (70) due to the string rotation. According to [5] this can be written as

$$\Delta M = -\frac{16\sigma^2 L(L+1)}{3(M_n^{(0)})^3}. \tag{113}$$

Let us note the main properties of the mass formula (111). First of all it has the minimal possible number of input parameters; those are **current** quark masses (defined at the appropriate scale of 1GeV), string tension, $\alpha_s(r)$ or equivalently Λ_{QCD} and the overall subtraction constant C_0 .

We **do not introduce constituent quark masses** and do not expand in inverse quark masses to get spin interaction, as it is common in relativistic quark models. In addition we take into account string rotation, which is not done in those models.

Moreover, our expression of the total mass M_n is the result of derivation from the first principles of QCD with all steps and approximations clearly visible, so that one can check and improve if need be. This is in contrast to the ad hoc model building principle.

Now we come to the confronting of our approach and first of all mass formula (111) with experiment and lattice data.

6 Spectrum of light mesons, hybrids and glueballs

6.1

The spectrum of mesons and glueballs (and of any two constituents connected by the string with spins and Coulomb force neglected) is given by the Hamiltonian (74).

The denominator in (74) is actually the moment of inertia of the system, comprising both quark (the μ term) and string (the ν term) contributions.

The eigenvalues of (74) have been found quasiclassically in [44] and given in Table 3 for the case of zero-mass quarks. For the case of two-gluon glueballs the corresponding eigenvalues are obtained by multiplication with the square root of Casimir factors ratio; since for the adjoint string $\sigma_{adj} = \sigma_{fund}\frac{C_2(adj)}{C_2(fund)} = \frac{9}{4}\sigma_{fund}$ In Fig. 1 shown are trajectories of eigenvalues of (74) as functions of L and n . The Regge slope is close (within 3%) to the string slope $(2\pi\sigma)^{-1}$. Note also the linear trajectories in n with approximately 2 times smaller slope.

The resulting spectrum for light-light mesons was found first in [34] and is close in basic features to that of Isgur and Godfrey [7] for $L = 0$, but differs for $L > 0$, since we take into account string rotation, and differs somewhat in spin splittings, since we have used for spin-dependent (SD) terms expressions derived from QCD (102-106), (110). In Fig.1 also shown is the experimental ρ type Regge trajectory, which has almost the same slope, but

shifted downwards. For this reason we introduce at this point (as in most models) the negative constant C_0 , as a surrogate of the nonperturbative selfenergy term for each quark, while we do not introduce such term for the valence gluon. The reason for this procedure and an estimate of this selfenergy will be given in the second part of lectures (published separately), where effects of chiral symmetry breaking are taken into account.

An example of the calculated spectrum of light–light mesons is given in Table 7 for $I = 1$ case and compared to experiment. It is seen that the overall agreement is reasonable and comparable to that of Isgur–Godfrey model [7]. Note, however, that in [7] there are 14 fitting parameters, while we have in our approach only 3: α_s , σ and C_0 . The most important fact is that spin–dependent potentials are exactly derived with masses $\mu_0, \bar{\mu}_0$ without any expansion in inverse mass powers assumed in all potential quark models; moreover $\mu_0, \bar{\mu}_0$ are computed and expressed through $\sqrt{\sigma}$.

Several words should be said about pion. The present approach as a whole is based on the assumption that spin corrections can be computed as a perturbation. This also implies smallness of chiral symmetry breaking effects. Now for the pion this is not valid, hyperfine correction is too large, and what is even worse, if one tries to treat the spin-spin term $-\frac{8\pi\alpha_s}{3\mu_0^2}\delta^{(3)}(\vec{r})$ to higher orders, then the minimization of the mass M_n (111) in μ_0 is no more possible, since at $\mu_0 \rightarrow 0$ the spin-spin term diverges. This happens only in the pionic channel and signals the instability of the vacuum and the onset of chiral symmetry breaking. Therefore pion should not be considered in the framework of the approach described.

For radially excited pion states the spin-spin correction is smaller and the present approach may be more reasonable. Some of these states are presented in Table 7.

6.2 Hybrids

Hybrids and glueballs are the most interesting examples where all advantages of our approach can be seen clearly. First of all this is the definite construction of the hybrid (and glueball) Green’s function (49) based on the background perturbation theory. Note the difference of our definition of hybrids from that of the flux-tube model; at the same time the structure of in and out hybrid states $\Psi_{in,f}$ is similar to that of the lattice QCD. Moreover, since for hybrids we do not introduce any new parameters (and effective mass of the gluon μ_g will be calculated through string tension), one can predict hybrid and glueball masses unambiguously, in this way seriously checking the whole formalism. The first studies of hybrid spectra in this method have been done in [52-54]. For later development using variational methods see [55].

Let us turn to the construction of the hamiltonian for the hybrid system. We start with the hybrid Green’s function and treating spin terms as perturbation, disregard in the first approximation the gluon spin term $2igF_{\mu\nu}$ in (9). Using FSR we get similarly to (57) the form

$$G_{hyb}(x, y) = \langle \text{tr} \Gamma^{(f)}(m - \hat{D}) \int_0^\infty ds \int_0^\infty d\bar{s} \int_0^\infty ds_g e^{-K - \bar{K} - K_g} (Dz)_{xy} (D\bar{z})_{xy} (Du)_{xy} \times \Gamma^{(i)}(\bar{m} - \hat{D}) W_{hyb} \rangle \quad (114)$$

where

$$W_{hyb} = (\Phi(x, y))_{\alpha\beta} t_{\beta\gamma}^a \hat{\Phi}_{ab}(x, y) t_{\delta\alpha}^b \Phi_{\gamma\delta}(y, x), \quad (115)$$

and $\Phi(x, y), (\Phi(y, x))$ are transporters (27) belonging to the quark (antiquark) Green’s function, while $\hat{\Phi}(x, y)$ is that of the gluon in the adjoint representation. At this point one can use the large N_c approximation, which yields accuracy around 10% in the most problems of QCD.

Then the gluon line can be replaced by the 'tHooft rule with a double $q\bar{q}$ line,

$$t_{\beta\gamma}^a \hat{\Phi}_{ab} t_{\delta\alpha}^b \rightarrow \Phi_{\beta\alpha}(x, y) \Phi_{\gamma\delta}(y, x) \quad (116)$$

and the vacuum average of W_{hyb} reduces to the product

$$\langle W_{hyb} \rangle = \langle W(C_1) \rangle \langle W(C_2) \rangle \quad (117)$$

where C_1, C_2 are adjacent contours made of quark (antiquark) trajectory and gluon trajectory.

The subsequent transformations with (114) are the same as in the $q\bar{q}$ case leading from (57) to (67).

We shall use only the simplest form of the Hamiltonian for zero angular momenta, equivalent to (70) and (112). In the case of the hybrid state it is

$$H_{hyb} = \frac{m_1^2}{2\mu_1} + \frac{m_2^2}{2\mu_2} + \frac{\mu_1 + \mu_2 + \mu_3}{2} + h_H - C_0(q\bar{q}g) \quad (118)$$

with

$$h_H = -\frac{1}{2m} \left(\frac{\partial^2}{\partial \xi^2} + \frac{\partial^2}{\partial \eta^2} \right) + \sigma |\mathbf{z}^{(1)} - \mathbf{z}^{(3)}| + \sigma |\mathbf{z}^{(2)} - \mathbf{z}^{(3)}|; \quad (119)$$

where we have defined c.o.m. coordinate and total effective mass respectively as

$$R_i = \sum_{k=1}^3 \frac{\mu_k z_i^{(k)}}{\mu}, \quad \mu = \sum_{k=1}^3 \mu_k \quad (120)$$

while Jacobi coordinates ξ_i, η_i , are expressed through those of q, \bar{q} : $z_i^{(1)}, z_i^{(2)}$ and of gluon $z_i^{(3)}$ as

$$\begin{aligned} z_i^{(3)} &= R_i - \sqrt{\frac{m(\mu_1 + \mu_2)}{\mu\mu_3}} \xi_i \\ z_i^{(1)} &= R_i + \sqrt{\frac{m\mu_3}{\mu(\mu_1 + \mu_2)}} \xi_i + \sqrt{\frac{m\mu_2}{\mu_1(\mu_1 + \mu_2)}} \eta_i \\ z_i^{(2)} &= R_i + \sqrt{\frac{m\mu_3}{\mu(\mu_1 + \mu_2)}} \xi_i - \sqrt{\frac{m\mu_1}{\mu_2(\mu_1 + \mu_2)}} \eta_i \end{aligned} \quad (121)$$

Here m is an arbitrary mass parameter. At this point one should comment on gluon exchanges between the valence gluon in the hybrid and quark (or antiquark). As we shall see in the next section, devoted to glueballs, a valence gluon does not have a color Coulomb interaction with another gluon or quark: the OGE diagrams existing in the lowest order do **not** sum up in the ladder-type series of the Coulomb interaction, since exchanged gluon and valence gluon are identical and moreover four-gluon vertex is also important. This is in contrast to the $q\bar{q}$ or qqq systems, where the Coulomb series occurs naturally as a first term in the cluster expansion series, see (81). The perturbative series for the gluon-gluon case is summed up in the Lipatov approach [56] and the result for the gluon ladder is strongly damped by the one-loop corrections. Therefore we disregard here the corresponding Coulomb terms for qg and $\bar{q}g$ systems.

The Hamiltonian (118) can be used in problems of two types. First, one can consider, as it is done on the lattice, [57], fixed (very heavy) quark and antiquark at a distance R from each other, and gluon in some angular momentum and spin state.

In this case one can define as in [57] the potentials $V_r(r)$ for the static $Q\bar{Q}$ pair at distance r with gluon in a state, which can be denoted as in the diatomic molecule, i.e. with projection of the total gluon momentum \mathbf{J} on the axis \mathbf{r} ,

$$\Lambda = \mathbf{J}\mathbf{r}/r, \quad \Lambda = 0, 1, 2, \dots(\Sigma, \Pi, \Delta, \Phi) \quad (122)$$

and combined operator of inversion w.r.t. midpoint of $Q\bar{Q}$ and charge conjugation $\eta_{cp} = 1(-1)$ denoted as $g(u)$. Σ can be also even (odd) w.r.t reflection in the plane of $Q\bar{Q}$, denoted as $+(-)$.

The Hamiltonian for the gluon in such two-center problem looks like

$$H_{Q\bar{Q}g} - H_{Q\bar{Q}} = \frac{\mu_3}{2} + \frac{\mathbf{p}^2}{2\mu_3} + \sigma|\mathbf{z}^{(3)} - \mathbf{z}_Q| + \sigma|\mathbf{z}^{(3)} - \mathbf{z}_{\bar{Q}}| + V_{LS} + \frac{3}{2} \frac{\alpha_s}{r} \quad (123)$$

where the spin-orbit term is similar to that in (101), while the Coulomb term is a result of subtraction from the color-octet repulsion $\frac{\alpha_s}{6r}$ in the $Q\bar{Q}g$ system of the attractive color-singlet term $-\frac{4\alpha_s}{3r}$.

The Hamiltonian (123) can be studied numerically.

A rough estimate of the eigenvalues of (123) is obtained when one expands string potentials in (123) assuming that gluon slightly vibrates around the midpoint of $Q\bar{Q}$, expanding the square roots.

Then the spectrum is

$$\Delta V_{Q\bar{Q}g}(r) = \left(\frac{4\sigma}{r}\right)^{1/3} \left(n + \frac{3}{2}\right)^{2/3} + \frac{3}{2} \frac{\alpha_s}{r}, \quad n = 0, 1, 2, \dots \quad (124)$$

A comparison of (124) with the lattice calculation [57] shows a good qualitative agreement.

We turn now to the real physical objects, $q\bar{q}g$ systems with light or heavy quarks. In this case one should take quark kinetic energies into account and consider $q\bar{q}g$ as a 3-body system with the Hamiltonian given in (118). The most efficient way to treat this problem is the hyperspherical expansion [58]. One defines the hyperradius ρ as

$$\rho^2 = \eta^2 + \xi^2, \quad (125)$$

and expands the wave function in a series

$$\Psi(\boldsymbol{\xi}, \boldsymbol{\eta}) = \sum_{K\nu n} \chi_{KN}(\rho) \Omega_{K\nu} \quad (126)$$

where $\Omega_{K\nu}$ is hyperspherical angular function [58], and ν denotes all quantum numbers in addition to the global momentum $K = 0, 1, 2, \dots$

Keeping only one harmonics with the given K , one obtains radial equation (neglecting for the moment Coulomb and spin-dependent terms)

$$\left[-\frac{d^2}{2md\rho^2} + W(\rho)\right]\chi_{Kn}(\rho) = \varepsilon_{Kn}\chi_{Kn}(\rho) \quad (127)$$

where

$$W(\rho) = \frac{\alpha(\alpha+1)}{2m\rho^2} + \sigma\rho \frac{32}{15\pi}(\alpha_{13} + \alpha_{23}) \quad (128)$$

and

$$\alpha = K + \frac{3}{2}, \quad \alpha_{i3} = \sqrt{\frac{m(\mu_i + \mu_3)}{\mu_i \mu_3}}, \quad i = 1, 2. \quad (129)$$

For an estimate with some 5% accuracy, one can find ε_{kn} by simply minimizing $W(\rho)$ in ρ .

Assuming now equal quark masses, $m_1 = m_2$ one could obtain $\mu_1 = \mu_2$, and taking the total hybrid mass as

$$M_{K_n} = \frac{m^2}{\mu_1} + \mu_1 + \frac{\mu_3}{2} + \varepsilon_{K_n} - C_0(q\bar{q}g) \quad (130)$$

and finding the minimal value ε_{K_n} from $W(\rho_0)$, one has

$$M_{K_n} = \frac{m_1^2}{\mu_1} + \mu_1 + \frac{\mu_3}{2} + \frac{3\sigma^{2/3}}{2\mu_{13}^{1/3}}\bar{C} - C_0(q\bar{q}g) \quad (131)$$

where $\bar{C} = (\frac{64}{15\pi})^{2/3}[\alpha(\alpha + 1)]^{1/3}$. It is reasonable to take $C_0(q\bar{q}g)$ the same as in the $q\bar{q}$ case since the constant term is due to quark selfenergy terms only.

In the limit of heavy mass $m_1 \gg \sqrt{\sigma}$, one get from minimization $\mu_1 \approx m_1$, and minimizing in μ_3 one obtains

$$M_{K_n} = 2m_1 + 2\sqrt{\sigma}\bar{C}^{3/4} - C_0(q\bar{q}g) \quad (132)$$

In particular, subtracting the heavy mass $2m_1 - C_0$ one gets

$$\Delta M = 2\sqrt{\sigma}\bar{C}^{3/4} = \begin{array}{l} 2.72\sqrt{\sigma} = 1.375\text{GeV}, \quad K = 0 \\ 3.44\sqrt{\sigma} = 1.7\text{GeV}, \quad K = 1 \end{array} \quad (133)$$

For light quarks one takes the same C_0 for a light hybrid as for the corresponding light meson. For the lowest exotic hybrid 1^{-+} one should take $K = 1$ ($L = 1$ for the gluon) and agreement with recent lattice calculation of the $b\bar{b}g$ mass excitation is very good, see Table 8.

6.3 Glueballs

This section is based on papers [59,60]. The $L = 0$ Hamiltonian for glueballs (neglecting spin and perturbative interaction) is obtained from that of $q\bar{q}$ system by replacing σ_{fund} by σ_{adj} .

$$H'_0 = \frac{\mathbf{p}^2}{\mu_0} + \mu_0 + \sigma_{adj}r \quad (134)$$

The value of σ_{adj} in (134) can be found from the string tension of $q\bar{q}$ system, since the Casimir scaling found on the lattice [33] predicts that

$$\sigma_{adj} = \frac{C_2(adj)}{C_2(fund)}\sigma_{fund} = \frac{9}{4}\sigma_{fund} \quad (135)$$

For light quarks the value of σ_{fund} is found from the slope of meson Regge trajectories and is equal to

$$\sigma_{fund} = \frac{1}{2\pi\alpha'} \approx 0.18\text{GeV}^2 \quad (136)$$

From that we find

$$\sigma_{adj} \approx 0.40\text{GeV}^2 \quad (137)$$

In what follows the parameter μ and its optimal value μ_0 , which enters in (134) play very important role. The way they enter spin corrections in (101) and magnetic moments shows that μ_0 plays the role of effective (constituent) gluon mass (or constituent quark mass in the equation for the $q\bar{q}$ system).

In contrast to the potential models, where the constituent mass of gluons and quarks is introduced as the fixed input parameter in addition to the parameters of the potential, in our approach μ_0 is calculated from the extremum of the eigenvalue of equation (134), which yields

$$\mu_0(n) = \sqrt{\sigma} \left(\frac{a(n)}{3} \right)^{3/4}, M_0(n) = 4\mu_0(n)$$

where $\sigma = \sigma_{adj}$ for gluons and $\sigma = \sigma_f$ for masses quarks, and $a(n)$ is the eigenvalue of the reduced equation $\psi'' + (a(n) - \rho - L(L+1)/\rho^2)\psi = 0$ The first several values of $a(n)$ and $\mu_0(n)$ are given in the Table 2, and will be used below.

Note that our lowest "constituent gluon mass" $\mu_0(n = L = 0) = 0.528 GeV$ (for $\sigma_f = 0.18 GeV$) is rather close to the values introduced in the potential models, the drastic difference is that μ_0 depends on n, L and grows for higher states.

From Table 1,2,3 and Fig. 1 one can see that mass spectra of the Hamiltonian (67) are described with a good accuracy by a very simple formula (a similar conclusion follows from calculations in [45])

$$\frac{M^2}{2\pi\sigma} = L + 2n_r + c_1 \quad (138)$$

where L is the orbital momentum, n_r -radial quantum number and c_1 is a constant ≈ 1.5 . It describes an infinite set of linear Regge-trajectories shifted by $2n_r$ from the leading one ($n_r = 0$). The only difference between light quarks and gluons is the value of σ , which determines the mass scale.

Thus the lowest glueball state with $L = 0, n_r = 0$ according to eqs. (6), (5) has $M^2 = 4.04 GeV^2$.

It corresponds to a degenerate 0^{++} and 2^{++} state.

$$M = 2.01 GeV \quad (139)$$

In order to compare our results with the corresponding lattice calculations [61-63] it is convenient to consider the quantity $\bar{M}/\sqrt{\sigma_f}$, which is not sensitive to the choice of string tension σ^2 . The spectrum of glueball states obtained in lattice calculations is given in the Table 9, where masses of glueballs for values of σ_f used in these calculations are given.

From these data we have for $L = 0, n_r = 0$ states the spin averaged mass

$$\frac{\bar{M}}{\sqrt{\sigma_f}} = \frac{M(0^{++}) + 2M(2^+)}{3} \frac{1}{\sqrt{\sigma_f}} \quad (140)$$

the value 4.61 ± 0.1 , which should be compared to our prediction $\bar{M}^{theor}(L = 0, n_r = 0)/\sqrt{\sigma_f} = 4.60$.

For radially excited states our theory predicts

$$\frac{\bar{M}^{theor}}{\sqrt{\sigma_f}}(L = 0, n = 1) = 7.0 \quad (141)$$

²Note that the value $\sigma_f \simeq 0.21 GeV^2$ used in lattice calculations differs by about 20% from the "experimental" value $\sigma_f = 0.18 GeV^2$.

Lattice data [61] give for this quantity

$$\frac{\bar{M}^{lat}}{\sqrt{\sigma_f}}(L = 0, n_r = 1) = 6.8 \pm 0.35 \quad (142)$$

For $L = 1, S = 1$ states one can define spin-averaged mass in a similar way

$$\frac{\bar{M}}{\sqrt{\sigma_f}} = \frac{M(0^{-+}) + 2M(2^{-+})}{3} \frac{1}{\sqrt{\sigma_f}} \quad (143)$$

lattice data [61-63] yield

$$\frac{\bar{M}^{lat}}{\sqrt{\sigma_f}}(L = 1, n = 0) = 6.36 \pm 0.5; \frac{\bar{M}^{lat}}{\sqrt{\sigma_f}}(L = 1, n = 1) = 8.1 \pm 0.5 \quad (144)$$

which is in a reasonable agreement with our prediction

$$\frac{\bar{M}^{theor}}{\sqrt{\sigma_f}}(L = 1, n_r = 0) = 5.95; \frac{\bar{M}^{theor}}{\sqrt{\sigma_f}}(L = 1, n_r = 1) = 8.0 \quad (145)$$

For $L = 2, n_r = 0$ the spin averaged state has

$$\frac{\bar{M}^{theor}(L = 2, n_r = 0)}{\sqrt{\sigma_f}} = 7.0 \quad (146)$$

Lattice data [61] exist only for 3^{++} state which yields $\frac{M(3^{++})}{\sqrt{\sigma_f}} = 7.7$. The overall comparison of spin-averaged masses computed by us and on the lattice shows a striking agreement.

Thus we come to the conclusion that the spin-averaged masses obtained from purely confining force with relativistic kinematics for valence gluons are in a good correspondence with lattice data, which implies that the dominant part of glueball dynamics is due to the QCD strings.

6.4 Spin splittings of glueball masses

Here we shall treat spin effects in a perturbative way, in the same manner, as it is done with spin effects in heavy and light quarkonia; a glance at the lattice results given in Table 9 tells that spin splittings in glueball states apart from $2^{++} - 0^{++}$ amount to less than 10-15% of the total mass, and hence perturbative treatment is justified to this accuracy level.

The two-gluon mass operator can be written as

$$M = M_0(n, L) + \mathbf{S}\mathbf{L}M_{SL} + \mathbf{S}^{(1)}\mathbf{S}^{(2)}M_{SS} + M_T, \quad (147)$$

where M_0 is the eigenvalue of the Hamiltonian $H' \equiv H_0 + \Delta H_{pert}$, and H_0 is given in (134), while ΔH_{pert} is due to perturbative gluon exchanges and as discussed in [60], gives a small correction, which will be omitted here.

To obtain three other terms in (147) one should consider averaging of the operators \hat{F} in (9) which enter in exponent for the Green's function and take into account that

$$-2i\hat{F}_{\mu\nu} = 2(\mathbf{S}^{(1)}\mathbf{B}^{(1)} + \tilde{\mathbf{S}}^{(1)}\mathbf{E}^{(1)})_{\mu\nu} \quad (148)$$

and similarly for the term in the integral $\int \hat{F} d\tau'$, with the replacement of indices $1 \rightarrow 2$. Here gluon spin operators are introduced, e.g.

$$(\mathbf{S}_m^{(1)})_{ik} = -ie_{mik}, \quad i, k = 1, 2, 3, \quad (\tilde{\mathbf{S}}_m^{(1)})_{i4} = -i\delta_{im} \quad (149)$$

Background gauge condition (46) allows to exclude $\mu = \nu = 4$, and hence $\tilde{\mathbf{S}}^{(1)}$ in (148). Since the structure of the term \hat{F} is the same as in case of heavy quark with the replacement of the heavy quark mass by the effective gluon parameter μ_0 (see (134)), one can use the spin analysis of heavy quarkonia done in [46,50], to represent the spin-dependent part of the Hamiltonian in the form similar to that of Eichten and Feinberg [51]

$$\begin{aligned} \Delta H_s = & \frac{\mathbf{S}\mathbf{L}}{2\mu_0^2} \left(\frac{2}{r} \frac{dV_1}{dr} + \frac{2}{r} \frac{dV_2}{dr} \right) + \frac{\mathbf{S}^{(1)}\mathbf{S}^{(2)}}{3\mu_0^2} V_4(r) + \\ & + \frac{1}{3\mu_0^2} (3(\mathbf{S}^{(1)}\mathbf{n})(\mathbf{S}^{(2)}\mathbf{n}) - \mathbf{S}^{(1)}\mathbf{S}^{(2)}) V_3(r) + \Delta V \end{aligned} \quad (150)$$

where $\mathbf{S} = \mathbf{S}^{(1)} + \mathbf{S}^{(2)}$, ΔV contains higher cumulant contributions (which can be estimated to be of the order of 10% of the main term in (150)).

The functions $V_i(r)$ are the same as for heavy quarkonia [48,50] except that Casimir operator is that of adjoint charges, the corresponding expressions of $V_i(r)$ in terms of correlators $D(x), D_1(x)$, are given in (46,50). Both D and D_1 are measured on the lattice [22-25] and D_1 is found to be much smaller than D . Therefore one can neglect the nonperturbative part of $V_3(r)$, while that of V_4 turns out to be also small numerically, $M_{SS}(\text{nonpert.}) < 30\text{MeV}$, and we shall also neglect it.

The only sizable spin-dependent nonperturbative contribution comes from the term $\frac{dV_i}{dr}$ (Thomas precession) and can be written asymptotically at large r as

$$\Delta H(\text{Thomas}) = -\frac{\sigma_{adj}}{r} \frac{\mathbf{L}\mathbf{S}}{2\mu_0^2} \quad (151)$$

Now we come to the point of perturbative contributions to spin splittings.

In heavy and light quarkonia these contributions are simply obtained from (102-106) substituting for D, D_1 their perturbative expressions to the order $O(\alpha_s)$ (109). In case of glueballs one should make replacement $C_2(\text{fund}) \rightarrow C_2(\text{adj})$ in (110) and in addition take into account two corrections due to the fact that *i*) valence and exchanged gluons are identical *ii*) there is 4-gluon vertex. These corrections have been taken into account in [64] and amount to some reduction of coefficients in (110).

The resulting matrix elements in (147) look like

$$M_{SL}^{(pert)} = \frac{3C_2(\text{adj})}{4\mu_0^2} \langle \frac{\alpha_s}{r^3} \rangle \quad (152)$$

$$M_{SS}^{(pert)} = \frac{5\pi C_2(\text{adj})}{3\mu_0^2} \langle \alpha_s \delta^{(3)}(r) \rangle \quad (153)$$

$$M_T^{(pert)} = \frac{C_2(\text{adj})}{\mu_0^2} \langle \frac{\alpha_s}{r^3} (3\mathbf{S}^{(1)}\mathbf{n}\mathbf{S}^{(2)}\mathbf{n} - \mathbf{S}^{(1)}\mathbf{S}^{(2)}) \rangle \quad (154)$$

From (153) one can see that M_{SS} can be written as

$$M_{SS} = \frac{5\alpha_s}{4\mu_0^2} |R(0)|^2 \quad (155)$$

To make simple estimates, we shall neglect first the interaction due to perturbative gluon exchanges between valent gluons. Indeed it was shown in [39] that this interaction cannot be written as Coulomb potential between adjoint charges, and comparison to perturbative Lipatov pomeron theory [56] shows that it is much weaker than Coulomb potential. Neglecting this interaction altogether, one gets the lower bound of spin-dependent effects, since all matrix elements, like $\langle \delta^{(3)}(r) \rangle$, $\langle \frac{1}{r} \rangle$, $\langle \frac{1}{r^3} \rangle$ are enhanced by attractive Coulomb interaction.

For purely linear potential one has simple relation, not depending on radial quantum number n_r [44,47]

$$|\Psi(0)|^2 = \frac{|R(0)|^2}{4\pi} = \frac{\mu_0 \langle V'(r) \rangle}{4\pi} = \frac{\mu_0 \sigma_{adj}}{4\pi} \quad (156)$$

Using (72,73), one obtains

$$M_{ss} = \frac{5\alpha_s \sigma_{adj}}{M_0} \quad (157)$$

and for $n_r = 0, 1$ and $\alpha_s = 0.3$ one obtains

$$M_{ss}(n_r = 0) = 0.3 GeV, M_{ss}(n_r = 1) = 0.20 GeV \quad (158)$$

For $M(0^{++})$ and $M(2^{++})$ one has the values given for the sake of comparison with lattice calculations in Table 9 for $\sigma_f = 0.23 GeV^2$ and $\alpha_s = 0.2(0.3)$

For $L > 0$ one needs to compute spin corrections M_{SL} and M_T . First of all one can simplify matter using the equation (it is derived in the same way, as (156) was derived in [47])

$$L(L+1) \langle \frac{1}{r^3} \rangle = \frac{\mu_0}{2} \langle V'(r) \rangle \quad (159)$$

For $V(r) = \sigma_{adj} r$ both $M_{SL}^{(pert)}$ and $M_T^{(pert)}$ are easily calculated and used in Table 9.

The estimate of $\Delta H(Thomas) = \frac{\vec{S}\vec{L}}{2\mu_0^2} \langle \frac{V_1+V_2}{r} \rangle$ is more cumbersome since this matrix element is very sensitive to the behaviour of $V_i(r)$ at small r , where the asymptotics (151) is not yet achieved. Therefore one has to use explicit expressions (102, 103) of V_1', V_2' through correlators D, D_1 (see [50] for details and discussion).

The resulting figures for ΔM_{thomas} are used in Table 9. Combining all corrections and values of M_0 from Table 2 one obtains glueball masses shown and compared with lattice data in Table 9 for $\sigma_f = 0.23 GeV^2$.

The general feature of spin-dependent contribution ΔH_s is that it dies out fast with the growing orbital or radial number, which can be seen in the appearance of the μ_0^2 factor in the denominator of (150).

Indeed, from (73) one can derive that $M_0 \approx 4\mu_0$ and therefore $\Delta H_s \sim \frac{1}{M^2(n,l)} \langle O(\frac{1}{r}) \rangle$, where O stands for terms like $const. \frac{1}{r}$ or $const' \cdot \frac{1}{r^3}$ (from perturbation theory). Hence spin splittings of the radial recurrence of states $0^{++}, 2^{++}$ or $0^{-+}, 2^{-+}$ should be smaller than the corresponding ground states. This feature is well supported by the lattice data in Table 9.

We end this section with the discussion of heavy-light mesons, which can be calculated also in the present approach, see [46]. While in [3] is given another and more exact approach

for heavy–light mesons, taking into account chiral symmetry breaking, here we shall only demonstrate that the present approach enables one not only reproduce the spectrum, but also calculate more delicate characteristics, e.g. decay constants f_m , $M = B, B_s, D, D_s$ and lepton width. These are characteristics computed in [46] and shown in Table 10. One can see a reasonable agreement of all entries with lattice data and experiment.

We do not touch in these lectures the topic of heavy quarkonia, which has been also extensively studied in the framework of the present approach [19,32], since this is the subject of lectures of F.J.Yndurain at this School [66].

7 Light–cone Hamiltonian and spectra for mesons.

In this chapter we follow mostly the work done in [41]. The light–cone description of the hadron wave functions is widely used, since it allows to get a direct connection to the parton model and its QCD improvements [67]. The latter however are mostly perturbative and nonperturbative contributions are introduced via OPE and QCD sum–rules. In this way the concept of the string – the main nonperturbative QCD phenomenon – is totally lost. On physical grounds it seems that the string is the essential ingredient of the dynamics for large ($r \geq 0.3 fm$) distances, and it would be interesting to understand its contribution to the light–cone wave functions, formfactors, structure functions etc.

In particular, what is the QCD string in the parton language? Should one associate it with the gluon contribution as an assembly of gluons compressed inside the string – or with the constituent quark mass?

There two contrasting points of view have been proposed already decades ago [68, 69]. In [68] the sea quarks and gluons enter as separate entities and one could associate the gluon distribution with the string in the same way as photons with the Coulomb field of the charge in the Williams–Weizsäcker method. In contrast to that in [69] the quarks have been considered as constituents with structure, and string does not appear separately. Recently a quantitative analysis was performed [70] of quark distribution in the pion starting from that in the nucleon and assuming the same internal structure of quarks in nucleon and in pion. It is still an open question how the structure of the constituent quarks is formed, and to which extent it can be explained by the adjacent piece of the string. This problem can be elucidated partly in the present approach, since our light–cone Hamiltonian contains the string on the light cone explicitly. It allows to separate the contribution of the string to the parton distribution, in particular to the momentum sum–rule. There is another source of structure in the constituent quark – chiral symmetry breaking which creates the chiral part of constituent quark. This problem will not be discussed below, see e.g. [3].

Let us make a few comments about the reasons why the light-cone dynamics is interesting to explore in QCD. One simple reason was stated in the beginning: it is to formulate in terms of parton language and therefore to single out the new nonperturbative contribution in the familiar parton picture. Second reason is quite general: the necessity of using Hamiltonians in moving frames to calculate observables, like form-factors or cross sections, where overlap integrals of eigenfunctions in different frames enter. An important advantage of the light–cone wave functions is that they allow to calculate formfactors and structure functions directly, without additional boosts, which typically are the dynamical ones, i.e. require the use of the exact Hamiltonian.

There is still another and deeper reason for using the light-cone formalism. It is based on the expectation [71] that the field theory in general has a more simple vacuum structure on the light-cone and in addition some classes of diagrams (containing backward-in-time motion) are suppressed. Hence one may expect that on the light-cone it is possible to choose the field degrees of freedom which are independent and simplest.

We consider the relativistic quark-antiquark pair with the masses m_1 and m_2 connected by the straight-line Nambu-Goto string with the string tension σ in 3+1 dimensional space-time.

Given a $q\bar{q}$ Green's function in the coordinate space $G(x\bar{x}; y\bar{y})$, where $x\bar{x}(y\bar{y})$ are final (initial) 4-coordinates of quark and antiquark, one can define the Hamiltonian H through the equation (in the euclidean space-time)

$$\frac{\partial G}{\partial T} = -HG \quad (160)$$

where T is an evolution parameter corresponding to some choice of a hypersurface Σ . In a particular case of the c.m. Hamiltonian the role of T is played by the center-of-mass euclidean time coordinate $T = (x_4 + \bar{x}_4)/2$ and the hypersurface Σ is a hyperplane $x_4 = \bar{x}_4 = \text{const}$.

With the notations for the vectors a_μ, b_μ

$$ab = a_\mu b_\mu = a_i b_i - a_0 b_0 = a_\perp b_\perp + a_+ b_- + a_- b_+,$$

$$a_\pm = \frac{a_3 \pm a_0}{\sqrt{2}},$$

one can define the hypersurface Σ through the $q\bar{q}$ coordinates z_μ, \bar{z}_μ as

$$z_+(\tau) = \bar{z}_+(\bar{\tau})$$

and the kinetic part of the action A

$$A = K + \bar{K} + \sigma S_{min},$$

has the form

$$\begin{aligned} K + \bar{K} &= \frac{1}{4} \int_0^s \dot{z}_\mu^2(\tau) d\tau + \frac{1}{4} \int_0^{\bar{s}} \dot{\bar{z}}_\mu^2(\bar{\tau}) d\bar{\tau} + \int_0^s m_1^2 d\tau + \int_0^{\bar{s}} m_2^2 d\bar{\tau} = \\ &= \int_0^T dz_+ \left[\frac{\mu_1}{2} (\dot{z}_\perp^2 + 2\dot{z}_-) + \frac{\mu_2}{2} (\dot{\bar{z}}_\perp^2 + 2\dot{\bar{z}}_-) + \frac{m_1^2}{2\mu_1} + \frac{m_2^2}{2\mu_2} \right] \end{aligned}$$

where we have defined

$$2\mu_1(z_+) = \frac{\partial z_+}{\partial \tau}; \quad 2\mu_2(z_+) = \frac{\partial \bar{z}_+}{\partial \bar{\tau}}$$

The minimal surface S_{min} is formed by connecting $z_\mu(z_+)$ and $\bar{z}_\mu(z_+)$ with the same value of the evolution parameter z_+ , i.e.

$$S_{min} = \sigma \int_0^T dz_+ \int_0^1 d\beta [\dot{w}^2 w'^2 - (\dot{w} w')^2]^{1/2}$$

where

$$w_\mu(z_+; \beta) = z_\mu(z_+) \beta + \bar{z}_\mu(z_+) (1 - \beta)$$

and dot and prime denote derivatives in z_+ and β respectively.

We now introduce "center-of-mass" and relative coordinates,

$$\dot{R}_\mu = x\dot{z}_\mu + (1-x)\dot{\bar{z}}_\mu, \quad \dot{r}_\mu = \dot{z}_\mu - \dot{\bar{z}}_\mu$$

where the variable x is defined from the requirement that the term $\dot{r}_\perp \dot{R}_\perp$ should be absent in the action. This yields:

$$x = \frac{\mu_1 + \int \nu \beta d\beta}{\mu_1 + \mu_2 + \int \nu d\beta} \quad (161)$$

Then for the Green function one obtains:

$$G(x\bar{x}; y\bar{y}) = \int D\mu_1(z_+) D\mu_2(z_+) D\nu DR_\mu Dr_\mu e^{-A}$$

where the action A

$$A = \frac{1}{2} \int dz_+ \left\{ \frac{m_1^2}{\mu_1} + \frac{m_2^2}{\mu_2} + a_1(\dot{R}_\perp^2 + 2\dot{R}_-) + a\dot{r}_\perp^2 + \int \frac{\sigma^2}{\nu} d\beta r_\perp^2 - \frac{(r_- + \dot{R}_\perp r_\perp + (\langle\beta\rangle - x)\dot{r}_\perp r_\perp)^2}{r_\perp^2 (\int \nu d\beta)^{-1}} - \frac{(\dot{r}_\perp r_\perp)^2 \int \nu (\beta - \langle\beta\rangle)^2 d\beta}{r_\perp^2} \right\}, \quad (162)$$

The following notation was used:

$$a_1 = \mu_1 + \mu_2 + \int_0^1 \nu(\beta) d\beta \quad (163)$$

$$a = \mu_1(1-x)^2 + \mu_2 x^2 + \int_0^1 \nu(\beta) (\beta - x)^2 d\beta \quad (164)$$

Integration over DR_μ leads to an important constraint:

$$a_1 = P_+$$

Furthermore we go over into the minkowskian space, which means that

$$\mu_i \rightarrow -i\mu_i^M, \quad \nu \rightarrow -i\nu^M, \quad A \rightarrow -iA^M$$

For the minkowskian action we obtain (omitting from now on the superscript M everywhere)

$$A^M = \frac{1}{2} \int dz_+ \left\{ -\frac{m_1^2}{\mu_1} - \frac{m_2^2}{\mu_2} + a\dot{r}_\perp^2 - \int \frac{\sigma^2 d\beta}{\nu} r_\perp^2 - \nu_2 \frac{(\dot{r}_\perp r_\perp)^2}{r_\perp^2} - \frac{\nu_0 a_1}{(\mu_1 + \mu_2) r_\perp^2} [r_- + (\langle\beta\rangle - x)\dot{r}_\perp r_\perp]^2 \right\}$$

To complete the Hamiltonian formulation of our problem we define canonical momenta for the coordinates \dot{R}_- and \dot{r}_- . As it was shown, canonically conjugated momentum to the \dot{R}_- is

$P_+ = a_1$. Situation with \dot{r}_- is more subtle. In order to clarify the situation let us start with the general form of the $q\bar{q}$ Green's function in the Feynman–Schwinger formalism

$$G(x, y) = \int ds d\bar{s} Dz D\bar{z} e^{-K-\bar{K}} \langle W(C) \rangle$$

to impose boundary conditions, one can rewrite $Dz D\bar{z}$ using discretization

$$\xi_n \equiv z(n) - z(n-1), \bar{\xi}_n = \bar{z}(n) - \bar{z}(n-1)$$

$$Dz D\bar{z} = \prod_{n, n'} d\xi_n d\bar{\xi}_{n'} dp dp' \times \\ \times \exp \left\{ ip \left(\sum \xi_n + X - Y \right) + ip' \left(\sum \bar{\xi}_{n'} + X - Y \right) \right\}$$

One can introduce the total and relative momenta

$$P = p + p', \quad q = \frac{p - p'}{2};$$

and $\dot{R} = \Delta R_n / \varepsilon$; $N\varepsilon = T$, one has

$$\xi_n x_n + \bar{\xi}_n (1 - x_n) = \Delta R_n$$

$$\xi_n - \bar{\xi}_n = \Delta r_n$$

Expressing $\xi_n, \bar{\xi}_n$ through $\Delta R_n, \Delta r_n$ and going over to the momentum representation of G one obtains

$$G(P) = \int dq \prod_{n, n'} d\Delta R_n d\Delta r_{n'} \times \\ \times \exp \left\{ iA + iP \sum_n \Delta R_n + i \sum_n \left(\frac{1}{2} P (1 - 2x) + q \right) \Delta r_n \right\}$$

where $A = \int_0^T d\tau \mathcal{L} = \int_0^T d\tau (K + \bar{K} - \sigma S_{min})$ One can now introduce the Hamiltonian form of the path integral via

$$\int Dx e^{i \int \mathcal{L} d\tau} = \int Dx Dp e^{ip_k \dot{x}_k - i \int \mathcal{H} d\tau}$$

and rewrite the first two exponents as

$$\exp \left\{ i \int P_i \dot{R}_i d\tau + i \int \left[\frac{1}{2} P_i (1 - 2x(\tau)) + q_i \right] \dot{r}_i d\tau \right\}$$

The term proportional q_i disappears because of boundary conditions $r_\mu(0) = r_\mu(T) = 0$, and one obtains

$$p_+ = \frac{1}{2} P_+ (1 - 2x), \quad [p_+, r_-] = -i$$

One can rewrite this in the form

$$P_+ r_- = i \frac{\partial}{\partial x}, \quad [P_+ r_-, x] = i$$

Separating out the center of mass motion one defines the Hamiltonian from the corresponding Minkowskian action A^M :

$$A^M = \int dz_+ L^M, \quad H = p_\perp \dot{r}_\perp - L^M \quad (165)$$

with $p_{\perp} = \partial L^M / \partial \dot{r}_{\perp}$.

After all one easily obtains the explicit form of the Hamiltonian

$$H = \frac{1}{2} \left\{ \frac{m_1^2}{\mu_1} + \frac{m_2^2}{\mu_2} + \frac{L_z^2}{a r_{\perp}^2} + \frac{(p_{\perp} r_{\perp} + \gamma r_-)^2}{\tilde{\mu} r_{\perp}^2} + \int \frac{\sigma^2}{\nu} d\beta r_{\perp}^2 + \frac{\nu_0 P_+}{\mu_1 + \mu_2} \frac{r_{\perp}^2}{r_{\perp}^2} \right\} \quad (166)$$

Let us remind, that μ_1, μ_2 are einbein fields, playing the role of P_+ momenta of the particles, $\tilde{\mu} = \mu_1 \mu_2 / (\mu_1 + \mu_2)$, $\nu_0 = \int_0^1 d\beta \nu(\beta)$ and $\nu(\beta)$ is the einbein field with the physical meaning of the P_+ -momentum, carried by the string. As it has been mentioned above, the Hamiltonian explicitly depends on $L_z^2 = \vec{p}_{\perp}^2 \vec{r}_{\perp}^2 - (\vec{p}_{\perp} \vec{r}_{\perp})^2$, the corresponding mass parameter is equal to (164):

$$a = \mu_1(1-x)^2 + \mu_2 x^2 + \int_0^1 d\beta \nu(\beta) (\beta-x)^2$$

The variable x in the above expression is the same as defined in (161):

$$x = \frac{\mu_1 + \langle \beta \rangle \nu_0}{P_+} \quad (167)$$

where

$$P_+ = \mu_1 + \mu_2 + \nu_0 \quad (168)$$

is the light-cone total momentum of the system. Also

$$\gamma = \nu_0 \left(\langle \beta \rangle - \frac{\mu_1}{\mu_1 + \mu_2} \right) \quad (169)$$

where $\langle \beta \rangle = \int_0^1 d\beta \beta \nu(\beta) / \int_0^1 d\beta \nu(\beta)$. It is easy to show, that in the limit $\sigma \ll m^2$ Hamiltonian turns out to have well known form:

$$H = \frac{1}{2P_+} \left(\frac{m_1^2}{x} + \frac{m_2^2}{1-x} \right) + \sigma \cdot |r| \quad (170)$$

Let us stress that separation of this kind cannot be done beyond nonrelativistic limit.

As the next step one should quantize the classical Hamiltonian function. Before doing it, one should choose the appropriate set of dynamical variables. Three einbein fields μ_1, μ_2, ν introduced above play different dynamical roles. In the nonrelativistic case $m_1, m_2 \gg \sqrt{\sigma}$ (and therefore for the free particles) the dependence of Hamiltonian (and wave functions) on ν can be correctly found by minimization procedure with ν taken as a classical variable. This is in its turn a consequence of the fact, that string in our approach is the minimal one – it has no internal degrees of freedom and may only stretch or rotate as a whole.

On another hand, μ_1 and μ_2 on the light cone play the role of legitimate quantum dynamical degrees of freedom and can be expressed through x and P_+ as in (168) and (167).

There are two canonically conjugated pairs in our problem: $\{\vec{p}_{\perp}, \vec{r}_{\perp}\}$ and $\{x, (P_+ r_-)\}$. We introduce also a new dimensionless variable \tilde{y} instead of ν : $\tilde{y}(\beta) = \nu(\beta) / P_+$. It satisfies the obvious condition: $0 < \tilde{y} < 1$. This variable depends on \vec{r}_{\perp} as well as on $(P_+ r_-)$. Rigorously

speaking one should extract this dependence by the minimization of the Hamiltonian with respect to \tilde{y} as it has been explained above. Instead an easier (however approximate) way is chosen. On physical grounds it can be shown that for small r_{\perp}^2 one has $\tilde{y}_0 = \int_0^1 \tilde{y} d\beta \sim \text{const} \cdot r_{\perp}^2$ so that linear string energy density \tilde{y}_0/r_{\perp}^2 stays finite if $r_{\perp}^2 \rightarrow 0$, and using this property one can reproduce the correct 1+1 limit, namely 't Hooft equation [72], from the 3+1 light-cone Hamiltonian (166) (see [41]). On the other hand, if distances are increasing, \tilde{y}_0 tends to some limiting value which is determined by the virial theorem arguments. So one can parameterize \tilde{y} introducing several parameters and replace the minimization in the functional sense by the ordinary minimization with respect to these parameters. We have chosen the simplest 2-parametric form for \tilde{y} :

$$\tilde{y} = \frac{yt}{1 + \alpha t} \quad (171)$$

where $t = r_{\perp}^2$ and y and α are free parameters. The requirement $0 < \tilde{y} < 1$ leads to the restriction $0 < y < \alpha$. Let us stress again that this parameterization is the matter of convenience and all physical results are determined from the requirement that every energy level should have its own minimum.

It is easy to see from (167), that the x -variable is the part of the total momentum, carried by the first quark itself and a part of the string, "belonging" to this quark. Rewriting (167) in the form:

$$\frac{\mu_1}{P_+} = x - \tilde{y}\langle\beta\rangle \quad ; \quad \frac{\mu_2}{P_+} = (1 - x) - \tilde{y}(1 - \langle\beta\rangle) \quad (172)$$

one can conclude, that for the given \tilde{y} the variable x may vary in the following limits:

$$\tilde{y}\langle\beta\rangle \leq x \leq 1 - \tilde{y}(1 - \langle\beta\rangle) \quad (173)$$

It is more convenient to make rescaling to a new variable ρ which varies from zero to unity:

$$x = \tilde{y}\langle\beta\rangle + (1 - \tilde{y})\rho \quad ; \quad 0 \leq \rho \leq 1 \quad (174)$$

The quantity we are really interested in is the mass operator squared:

$$\hat{M}^2 = 2 \hat{H} P_+ \quad (175)$$

Using definition (167) we obtain the following form for M^2 :

$$\begin{aligned} M^2 = & \left\{ \frac{m_1^2}{x - \tilde{y}_0\langle\beta\rangle} + \frac{m_2^2}{1 - x - \tilde{y}_0(1 - \langle\beta\rangle)} + \frac{L_z^2}{\tilde{c} r_{\perp}^2} + \right. \\ & + \left[\frac{1}{x - \tilde{y}_0\langle\beta\rangle} + \frac{1}{1 - x - \tilde{y}_0(1 - \langle\beta\rangle)} \right] \times \\ & \quad \times \frac{[p_{\perp} r_{\perp} + \tilde{\gamma}(P_+ r_-)]^2}{r_{\perp}^2} + \\ & \left. + \int \frac{\sigma^2}{\tilde{y}} r_{\perp}^2 d\beta + \frac{\tilde{y}_0}{1 - \tilde{y}_0} \frac{(P_+ r_-)^2}{r_{\perp}^2} \right\} \end{aligned}$$

here

$$\tilde{c} = (x - \tilde{y}_0\langle\beta\rangle)(1 - x)^2 +$$

$$[1 - x - \tilde{y}_0(1 - \langle\beta\rangle)]x^2 + \int_0^1 \tilde{y}(\beta - x)^2 d\beta$$

and

$$\tilde{\gamma} = \frac{\tilde{y}_0}{1 - \tilde{y}_0} (\langle\beta\rangle - x)$$

As it was mentioned above, it is more convenient to express M^2 through a new variable ρ :

$$\rho = \frac{1}{1 - \tilde{y}_0} (x - \tilde{y}_0 \langle\beta\rangle)$$

In terms of this variable one obtains:

$$\begin{aligned} M^2 = & \frac{1}{1 - \tilde{y}_0} \left\{ \frac{m_1^2}{\rho} + \frac{m_2^2}{1 - \rho} + \frac{L_z^2}{\tilde{c} t} + \right. \\ & + \left(\frac{1}{\rho} + \frac{1}{1 - \rho} \right) \times \frac{[p_\perp r_\perp + \tilde{\gamma}(P_+ r_-)]^2}{t} + \\ & \left. + (1 - \tilde{y}_0) \int \frac{\sigma^2}{\tilde{y}} t d\beta + \frac{\tilde{y}_0 (P_+ r_-)^2}{t} \right\} \end{aligned} \quad (176)$$

where the notation $t = r_\perp^2$ was used.

Quantization of the above expression is done according to the canonical commutation relations:

$$\begin{aligned} \{p_\perp^k, r_\perp^j\} &= -i\delta^{kj} \\ \{x, (P_+ r_-)\} &= -i \end{aligned}$$

We are looking for the wave function of the problem given in the mixed coordinate – momentum representation $\psi = \psi(\rho, t)$, so one has to substitute into (176) the operators:

$$(P_+ r_-) = i \left(\frac{1}{1 - \tilde{y}_0} \right) \frac{\partial}{\partial \rho} \quad ; \quad p_\perp^k = -i \frac{\partial}{\partial r_\perp^k}$$

The important point is the operator ordering. We use the Weil ordering rule, i.e.

$$AB \rightarrow \frac{1}{2}(\hat{A}\hat{B} + \hat{B}\hat{A})$$

for any noncommuting operators A and B . Let us notice that \tilde{y} explicitly depends on t according to (171) and hence should also be differentiated during the ordering procedure. The final result for the operator \hat{M}^2 may be found by the straightforward calculations, it is

$$\begin{aligned} \hat{M}^2 = & A_1 \frac{\partial^2}{\partial t^2} + A_2 \frac{\partial^2}{\partial \rho^2} + A_3 \frac{\partial^2}{\partial t \partial \rho} + \\ & + A_4 \frac{\partial}{\partial t} + A_5 \frac{\partial}{\partial \rho} + A_6 \end{aligned} \quad (177)$$

where A_i are expressed through ρ, t, y , (see [41] for more details).

We have chosen six sets of quark mass parameters, including 4 sets of equal masses and 2 sets of unequal masses in the interval from 0 to 5 GeV. The values of parameters y, α, ϵ

are obtained by minimization procedure as explained above. The eigenstates obtained by our numerical procedure are shown in Fig.2.

Let us first discuss the light–cone spectrum. The Hamiltonian (166) depends explicitly on L_z , whereas the Lorentz–invariance requires that masses do not depend on L_z , but depend on L . Consequently one expects that the lowest state for $L_z = 0$ corresponds to $L = 0$, while the next state with $L_z = 0$ corresponds to $L = 1$ and must be degenerate in mass with the state $L_z = 1, L = 1$. This is clearly seen in the data.

At this point one should take into account another degeneration – the dynamical one, and to this end discuss first center–of–mass spectrum, obtained from the c.m. Hamiltonian [67]. The c.m. Hamiltonian for $L = 0$ reduces to the so–called spinless Salpeter equation [71] which was actually solved by us. The approximate form of the spectrum can be represented as:

$$\left(M^{(0)}(L, N_r)\right)^2 \cong 2\pi\sigma \left(2N_r + \frac{4}{\pi}L + \frac{3}{2}\right) \quad (178)$$

For $L > 0$ one should take into account the string contribution, absent in spinless Salpeter equation but present in the Hamiltonian [67]. This correction is done in (113). The corrected masses, $M(L, N_r) = M^{(0)} + \Delta M$ are shown in Fig.2. Now one can see that there is an approximate degeneration in mass $M = M^{(0)} + \Delta M$ of states when one replaces one unit of N_r by two units of L . The same type of approximate mass degeneration is seen in the light–cone spectrum – compare e.g. the states with $(N_r, L, L_z) = (1, 0, 0)$; $M_{LC} = 2.25$ and $(0, 2, 0)$; $M_{LC} = 2.28$.

In Fig.2 this degeneration is visualized as the fact that masses appear on the vertical lines. This degeneration is a dynamical one and is a characteristic feature of nonrelativistic oscillator. In our relativistic case it reveals a new string–like symmetry, typical for the QCD string spectrum [54].

Let us now compare the light–cone and the center–of–mass spectrum. One could expect the coincidence up to an overall shift due to the different treatment of Z –graphs in two systems. In the c.m. Hamiltonian these Z –graphs are presented but supposed to be unimportant on the grounds, that the backtracking of a quark in time necessarily brings about a folding in the string world sheet which costs a large amount of action and is therefore suppressed. The situation is different in the light cone – it is general belief that Z –graphs are absent here. One also expects that the Z –graphs (and the overall shift) should decrease if quark masses are increasing.

The comparison of the spectra can be made from Fig. 2. One can see indeed some overall shift down in the c.m. spectrum by some 0.1 GeV and otherwise the masses coincide within the accuracy of computation. This fact is highly nontrivial since two quantum Hamiltonians (the light–cone and center–of–mass ones) are different, they cannot be obtained from each other by a simple boost or other simple transformation. The light–cone Hamiltonian is rather complicated and it took the authors more than a year to get reasonable numerical results for it.

We have also checked the quark mass dependence of the overall shift of spectra and proved that it drops sharply with the quark mass increasing supporting the idea, that the shift is due to different treatment of Z graphs (or self energy graphs). This fact also confirms, that the shift is not a consequence of some systematic errors of our procedure.

We now turn to eigenfunctions. One expects in this case two types of excitation: the radial one leading to new nodes on ρ coordinate and similar to the 1+1 excited states and the r_\perp –excitation which causes nodes in the t –coordinate and associated with the orbital excitation. This is clearly seen in Fig. 3, where (a) refers to the ground state, (b) – to the orbital and (c) – to the radial excitation. A more complicated example, combining both types of excitation is given in Fig. 3 (d).

As the next illustration we show in Fig. 4 the case of two heavy quarks, demonstrating two types of excitation and also a new feature – the actual region of parameters is squeezed to a small region near $\rho = 1/2$.

At this point it is important to find connection of our light–cone wave function to the nonrelativistic one, usually defined in the c.m.. In [5] it was demonstrated that this connection can be established only when both quarks are heavy, $m_1, m_2 \gg \sqrt{\sigma}$. In this case $\tilde{y} \ll 1$ (as can be found by direct minimization of the Hamiltonian (166)) – the string transforms into the potential and loses its material and momentum contents. One can introduce as in [5] the relative momentum p_z and relative coordinate r_z :

$$p_z = (m_1 + m_2) \left(x - \frac{m_1}{m_1 + m_2} \right) \quad (179)$$

$$r_z = \frac{P_+ r_-}{m_1 + m_2} \quad (180)$$

and the M operator can be written as:

$$M \approx m_1 + m_2 + \frac{1}{2\tilde{m}} (\vec{p}_\perp^2 + \vec{p}_z^2) + \sigma \sqrt{r_\perp^2 + r_z^2} \quad (181)$$

Hence one can write the momentum–space nonrelativistic wave function $\Psi(\vec{p}^2)$ directly through the light–cone variables:

$$\Psi(\vec{p}^2) = \Psi \left[p_\perp^2 + (m_1 + m_2)^2 \left(x - \frac{m_1}{m_1 + m_2} \right)^2 \right] \quad (182)$$

This representation is valid in the large mass limit $m_i \gg \sqrt{\sigma}$ stated above and in addition near the center of the x –distribution, i.e. when $|x - m_1/(m_1 + m_2)| \ll 1$. The width of the peak in x variable is proportional to $(m_1 + m_2)^{-2}$ and is very narrow for heavy quarks. The form (179) is not correct for x at the ends of the interval, i.e. $x = 0, 1$ (remember that for large m_i the extremum value of \tilde{y} tends to zero and $x = \rho$ changes in the interval $[0, 1]$). Indeed the exact wave function as discussed in Section 4 vanishes linearly at $x = 0, 1$, while the r.h.s of (182) stays nonzero. Moreover, the Jacobean \mathcal{J} of the phase space $d^3p = \mathcal{J} dx d^2p_\perp$ is constant $\mathcal{J} = m_1 + m_2$ and does not change this conclusion.

The correspondence of the c.m. and light–cone wave functions is lost if quark masses m_i are of the order of $\sqrt{\sigma}$ or less. The physical reason is that the role of dynamics is now 100% important and the dynamics is different in different frames: the light–cone Hamiltonian and wave functions are connected with those of the center–of–mass by a dynamical transformation, which includes nonkinematical Poisson operators. Hence one cannot hope to obtain one wave function from another using only transformation including the kinematical (free) part of the operator M^2 . Moreover, a glance at the operator M^2 in (166) helps to realize that the separation of M^2 into the purely kinetic part (containing only momentum and masses) and purely potential one (containing only relative coordinates) is impossible at all: e.g. the string enters through the term $(P_+ r_-)^2$ and mixed terms like $p_\perp r_\perp$ are present everywhere. This circumstance limits the use of simple recipes known in literature [73], which connect the c.m. and light–cone wave functions. In particular, the ansatz for p_z suggested in [73] and used for equal quark masses

$$p_z = \sqrt{\frac{m^2 + k_\perp^2}{x(1-x)}} \left(x - \frac{1}{2} \right) \quad (183)$$

coincides with our form (180) rigorously derived in [40] only for large m , $m \gg \sqrt{\sigma}$ and x in the narrow region around $x = 1/2$ but differs at the tails of the wave function. For light quark masses, $m \leq \sigma$ and small p_\perp the relation (183) yields incorrect results which can be seen in the almost constant behaviour in the interval $[0,1]$ of the light-cone wave function, produced by the insertion of (183) into the c.m. wave function, typically

$$\psi(\vec{p}^2) \sim \exp(-a^2\vec{p}^2) \rightarrow \exp(-a^2[p_\perp^2 + \frac{m^2 + p_\perp^2}{x(1-x)}(x - \frac{1}{2})^2])$$

is insensitive to x for $m, p_\perp \rightarrow 0$, whereas the exact light-cone wave function is decreasing as $x(1-x)$, see Fig. 5.

At the same time for heavy quark masses, $m \gg \sqrt{\sigma}$ the two functions, one transformed by (183) from the c.m. and another is a genuine light-cone wave-function solution of (177), are very close to each other.

We now turn to the formfactor of computed states. The main feature is a very slow decrease of $F(q^2)$ with q^2 which signals in particular a small radius of states. Indeed the values of $\sqrt{\langle r^2 \rangle}$ are too low ($\sim 0.338 fm$ for massless quarks). This fact is in agreement with the earlier c.m. calculations of [74].

Finally we turn to the quark-distribution function $q(\rho)$. It is computed through the light-cone wave-function $\psi(\rho, t)$ using the relation $q(\rho) = \pi \int_0^\infty |\Psi(\rho, t)|^2 dt$ and shown in Fig. 6. One can see the symmetric behaviour of $q(\rho)$ with respect to reflection $\rho \rightarrow 1 - \rho$. At the ends of the interval $q(\rho)$ vanishes like ρ^2 and $(1 - \rho)^2$, in the agreement with the $1/q^3$ behaviour of the formfactor at large q due to the Drell-Yan-West relations [75].

Note the narrowing of the peak in $q(\rho)$ in Fig. 6 for increasing quark masses.

The main physical idea of our approach is that the most part of nonperturbative dynamics in QCD is due to the QCD string, and the latter is described by the Nambu-Goto part of the Hamiltonian, which was written before in the c.m. [5] as well as in the light-cone coordinates [40].

Only valence part of the Fock's column was considered above in the paper, also for simplicity spins and perturbative gluon exchanges are neglected. To do the systematic comparison with experiment all these three simplifications should be eliminated. Let us discuss their effect point by point. The higher Fock states are necessary to reproduce the Regge behaviour of $q(x) \sim x^{-\alpha_\rho(0)}$ at small x (and at $x \rightarrow 1$ for quark distributions of hadrons in high-energy scattering). Here comes the first crucial point; to be answered in the second part of these lectures, what is the QCD reggeon?

In our method the higher Fock states, constituting the QCD reggeon, correspond to several gluons propagating in the nonperturbative background and therefore confined to the excited Nambu-Goto surface [2]. These states are in one-to-one correspondence with the excited Nambu-Goto string states. This is the picture at large distances; at small distances smaller than the vacuum correlation length (width of the Nambu-Goto string) $T_g \sim 0.2 fm$, the string disappears and the usual perturbative gluon exchanges reappear.

The effect of spin of light quarks is highly nontrivial [3]. It leads to the creation of the new vertex, which yields the constituent quark structure. Physically one may imagine this structure as being due to the light-quark walks around the end of the string.

Having said all this, what are the lessons of the present work and of its possible development?

The first lesson is that valence quark component can be successfully dynamically computed on the light cone; the minimal string on the light cone is physically and mathematically well

defined. The structure of the spectrum obtained on the light cone for the first time reasonably coincides with that of the c.m. Hamiltonian for the string with quarks. Effects of Z-graphs are estimated to be less than 12% even for light quarks. Moreover, the nonperturbative wave function obtained directly on the light cone allows to calculate nonperturbative contributions to the formfactor and structure function.

The second lesson is that the formfactor computed directly on the light cone is close to of c.m. for small q , but is systematically above the c.m. formfactor for larger q . This is not surprising, since in the light-cone formfactor there is a mechanism of the "redistribution" of the momentum q between the quarks, since q enters the light-cone formfactor multiplied with $(1-x)$, so that the larger q , the smaller is $(1-x)$ and the wave function does not decrease too fast. Physically it means that at large q the configuration survives where the spectator quark gets as little momentum as possible so that it can be easily turned together with the active quark. This is exactly what is called the Feynman mechanism [76].

The third lesson is that the minimal string plays only a passive role on the light cone, namely it participates in sharing of the total momentum and carries the part equal to $\langle \tilde{y} \rangle$, but it does not produce the x -distribution in structure function, which could simulate the gluonic structure function. The reason is that the string variable – the einbein field ν – is quasiclassical and has no dispersion.

The value of $\langle \tilde{y} \rangle$ computed according to relation $\langle \tilde{y} \rangle = \pi \int_0^\infty \int_0^1 |\tilde{\Psi}(\rho, t)|^2 d\rho dt$ depends on quark masses and is equal to 0.22 for massless quarks. It is reasonable that $\langle \tilde{y} \rangle = 0.22$ is smaller than the experimental value of overall gluon momentum, 0.55, since in our picture the difference should be filled in by higher Fock components.

The fourth lesson comes from the comparison of the computed quark distribution, with the experimental data for the pionic structure function [77]. Behaviour of $q(\rho)$ at small ρ and small $(1-\rho)$ is symmetric in Fig.6, while in reality $q(x)$ should rise at small x like $x^{-\alpha_\rho(0)} \sim x^{-0.5}$ (we neglect at this point the difference between x and ρ , which is due to $\langle \tilde{y} \rangle$). This peak at the small x should be filled in by the contribution of higher Fock components, containing additional gluons on the string, as was discussed above. The behaviour of $q(\rho)$ at $\rho = 1$, which is calculated to be $(1-\rho)^2$ will be also changed into $(1-\rho)$ due to gluon exchanges, which account for the formfactor asymptotic $1/q^2$ at large q , and the Drell-Yan-West duality ensure the $(1-\rho)$ behaviour around $\rho = 1$.

Finally, the formfactor calculated above in the paper, shows too little radius of the "pion" $\langle r^2 \rangle \approx (0.34 fm)^2$ as compared with the experimental one $\langle r^2 \rangle \simeq (0.67 fm)^2$. This fact is in qualitative agreement with other calculations, where the c.m. wave-function was used [74], and some authors assumed as in [70] that quarks have "internal" structure and their own radius which should be added to the "body radius" to reproduce the experimental value. This fact of small body radius seems to be a necessary consequence of the simple string + point-like quarks picture, and probably cannot be cured by the higher Fock components; in the second part of lectures we shall come to this point from another direction.

8 Conclusions

As one can see from previous chapters, the simple relativistic string Hamiltonian (111-112) and its extension to the hybrid and glueball case works surprisingly well and describes quantitatively the observed meson spectrum and calculated on the lattice spectrum of hybrids and glueballs.

This implies that confinement in the form of the thin string is the basic element of the strong interaction, and for the most hadrons this is enough to reproduce main features like masses, decay constants, magnetic moments etc. Last years there appeared new successful applications of the method to the polarizability of mesons [78], to the description of nucleons [79] and to the calculation of the nonperturbative correlation masses in $SU(2)$ -Higgs model [80]. Analysis of heavy quarkonia, sensitive to small distances adds to this picture two elements: one needs to know one-loop corrections to spin-dependent forces and small distance behaviour of NP forces [19], [30]. However the world of Nambu-Goldstone bosons and chiral symmetry breaking (CSB) phenomena was completely omitted in the previous material for the lack of space. A new approach based on the analysis of the heavy light system [3], allows to formulate dynamical equations for mesons and baryons [65] in this case, taking into account CSB. Simultaneously one can calculate in the method the NP self-energy of the quark (constant C_0 subtracted from the mass eigenvalue in (112)), and consider spin effects not assuming its smallness. This part of material will be published separately as a second part of lectures.

The author is grateful to A.B.Kaidalov, Yu.S.Kalashnikova, F.J.Yndurain for discussions and to the Organizing Committee and Professor Lidia Ferreira for the effective organization and warm hospitality at the XVII International School.

References

- [1] Yu.A.Simonov, Physics-Uspekhi, **39** (1996) 313
- [2] Yu.A.Simonov: in Lecture Notes in Physics, Springer Verlag, v. 479
- [3] Yu.A.Simonov, Phys. At. Nucl. **60** (1997) 2252, hep-ph/9704301
- [4] Yu.A.Simonov, Phys. Lett. **B226** (1989). for a review see Yad. Fiz. **54** (1991) 192
- [5] A.Yu.Dubin, A.B.Kaidalov and Yu.A.Simonov, Phys. Lett. **B323** (1994) 41; Yad. Fiz. **56** (1993) 213
- [6] D.R.Stanley and D.Robson, Phys. Lett. **B45** (1980) 235
P.Cea, G.Nardulli and G.Preparata, Z.Phys. **C16** (1982) 135; Phys. Lett. **B115** (1982) 310; J.Carlson et al. Phys. Rev **D27** (1983) 233
- [7] N.Isgur and S.Godfrey, Phys. Rev. **D32** (1985) 189
- [8] J.L.Basdevant, S.Boukraa, Z.Phys. **C28** (1983) 413
- [9] Yu.A.Simonov, Phys. At. Nucl. **61** (1998) 855, hep-ph/9712250
- [10] Private correspondence to the author, for more details see [2]
- [11] Yu.A.Simonov, Yad. Fiz. **58** (1995) 113; JETP Lett. **57** (1993) 513
- [12] A.M.Badalian and Yu.A.Simonov, Phys. At. Nucl. **60** (1997) 630
- [13] M.Peter, Phys. Rev. Lett. **78** (1997) 602, Nucl. Phys. **B501** (1997) 471;
Y.Schroeder, Phys. Lett. **B 447** (1999) 321

- [14] G.S.Bali, hep-ph/9905387
- [15] S.P.Booth et al, Phys. Lett. **B294** (1992) 385; G.S.Bali and K.Schilling, Phys. Rev. **D47**(1993) 661, Nucl. Phys. B (Prec. Suppl.) 34 (1994) 147
- [16] A.C.Mattingly and P.M.Stevenson, Phys.Rev. **D 49** (1994) 437
- [17] D.V.Shirkov and I.L.Solovtsov, Phys. Rev. Lett. **79** (1997) 1209
- [18] A.M.Badalian, Phys. At.Nucl. **60** (1997) 1003 (Yad. Fiz. **60** (1997) 1122), hep-lat/9704004
- [19] A.M.Badalian and V.L.Morgunov, Phys. Rev. D, hep-ph/9901430
- [20] I.Aref'eva, Theor Math. Phys. **43** (1980) 353;
N.Bralic, Phys. Rev. **D22** (1980) 3090;
Yu.A.Simonov, Sov.J.Nucl. Phys. **50** (1989) 134;
M.Mirayama, S.Matsubara, hep-th/97 12120
- [21] N.G.Van Kampen, Stochastic Processes in Physics and Chemistry, North-Holland, 1984
- [22] A.Di Giacomo and H.Panagopoulos, Phys. Lett. **B285** (1992) 133
- [23] A.Di Giacomo, E.Meggiolaro and H.Panagopoulos, Nucl. Phys. **B483** (1997) 371
- [24] M.D'Elia, A.Di Giacomo and E.Meggiolaro, Phys. Lett. **B408** (1997) 315
- [25] G.S.Bali, N.Brambilla and A.Vairo,Phys. Lett. **B421** (1998) 265
- [26] L. Del Debbio, A.Di Giacomo and Yu.A.Simonov, Phys. Lett. **B332** (1994) 111
- [27] V.Marquard and H.G.Dosch, Phys. Rev. **D35** (1987) 2238
- [28] H.G.Dosch and Yu.A.Simonov, Phys. Lett. **B 205** (1988) 339
- [29] M.Eidemuelller, H.G.Dosch and M.Jamin hep-ph/9908318
- [30] Yu.A.Simonov, JETP Lett. **69** (1999) 505, Phys. Rep. **320** (1999) 265
- [31] R.Akhoury and V.I.Zakharov, Phys. Lett. **B438** (1998) 165
K.G. Chetyrkin, S, Narison and V.I.Zakharov, hep-ph/9811275
- [32] A.M.Badalian and V.P.Yurov, Yad.Fiz. **51** (1990) 1368; **56** (1993) 239
- [33] S.Deldar, hep-lat/9809137
G.Bali, hep-lat/9908021
- [34] Yu.A.Simonov, Yad. Fiz. **54** (1991) 192
- [35] N.Isgur and J.E.Paton, Phys. Lett. **124B** (1983) 247, Phys. Rev. **D31** (1985) 2910
N.Isgur, R.Kokoski, J.E.Paton, PRL **54** (1985) 869
T.Barnes, F.E.Close, E.S.Swanson, Phys. Rev. **D52**(1995) 5242
- [36] Yu.A.Simonov, Nucl. Phys. **B307** (1988) 512

- [37] Yu.A.Simonov and J.A.Tjon, Ann. Phys. (NY) **228** (1993) 1
- [38] Yu.A.Simonov, Phys. Lett. B (in press), hep-ph/9904431
- [39] A.B.Kaidalov and Yu.A.Simonov, hep-ph/9911291
- [40] A.Yu.Dubin, A.B.Kaidalov and Yu.A.Simonov, Phys. Lett. **B343** (1995) 360; Yad. Fiz. **58** (1995) 348
- [41] V.L.Morgunov, V.I.Shevchenko and Yu.A.Simonov, Phys. Lett. **B 416** (1998) 433; Yad. Fiz. **61** (1998) 739
- [42] A.M.Polyakov, Gauge fields and strings, Harwood Academic, 1987;
A.Yu.Dubin, JETP Lett. **56** (1992) 545
Yu.S.Kalashnikova, A.V.Nefediev, Phys. At. Nucl. **60** (1997) 1389; **61** (1998) 785
- [43] V.L.Morgunov, A.V.Nefediev and Yu.A.Simonov, Phys. Lett. **B459** (1999) 653
- [44] E.Eichten et al., Phys. Rev. **D17** (1978) 3090
- [45] Dan la Course and M.G.Olsson, Phys. Rev. **D39** (1989) 2751; C.Olsson, and M.G.Olsson, MAD/PH/761 (1993); M.G.Olsson, Nuovo Cim. **107 A** (1994) 2541
- [46] Yu.A.Simonov, Z.Phys. **C53** (1992) 419
- [47] W.Lucha, F.F.Schoeberl and D.Gromes, Phys. Rep. **200** (1991) 127
- [48] Yu.A.Simonov, Nucl. Phys. **B324** (1989) 67
- [49] Yu.A.Simonov, Spin interactions of light quarks, preprint ITEP 97-89 (unpublished)
- [50] A.M.Badalian and Yu.A.Simonov, Phys. At. Nucl. **59** (1996) 2164
- [51] E.Eichten and F.L.Feinberg, Phys. Rev. **D23** (1981) 2724
- [52] Yu.A.Simonov in: Proceeding of the Workshop on Physics and Detectors for DAΦNE, Frascati, 1991
- [53] Yu.A.Simonov, Nucl. Phys. B (Proc. Suppl.) **23 B** (1991) 283
- [54] Yu.A.Simonov in: Hadron-93 ed. T.Bressani, A.Felicielo, G.Preparata, P.G.Ratcliffe, Nuovo Cim. **107 A** (1994) 2629
- [55] Yu.S.Kalashnikova, Yu.B.Yufryakov, Phys. Lett. **B359** (1995) 175; Yu.Yufryakov, hep-ph/9510358
- [56] V.S.Fadin, E.A.Kuraev, L.N.Lipatov, Sov. Phys. JETP **44** (1976) 443, **45** (1977) 199;
Y.Y.Balitskii, L.N.Lipatov, Sov.J. Nucl. Phys. **28** (1978) 822;
L.N.Lipatov, Nucl. Phys. **B 365** (1991) 614, Sov. Phys. JETP **63** (1986) 904
- [57] K.J.Juge, J.Kuti and C.Morningstar, hep-lat/9809015

- [58] Yu.A.Simonov, *Yad. Fiz.* **3** (1966) 630;
A.M.Badalian and Yu.A.Simonov, *Yad.Fiz.* **3** (1966) 1032;
F.Calogero, Yu.A.Simonov, *Phys. Rev.* **183** (1968) 869
- [59] Yu.A.Simonov, *Phys. Lett.* **B249** (1990) 514
- [60] E.L.Gubankova and A.Yu.Dubin, *Phys. Lett.* **B334** (1994) 180
- [61] C.Morningstar, M.Peardon, hep-lat/9901004, *Nucl. Phys. B (Proc. Suppl.)* 63 A-C(1988) 22
- [62] M.Teper, hep-th/9812187
- [63] G.Bali et al. (UKQCD Collaboration), *Phys. Lett.* **B309** (1993) 378
G.Bali, hep-lat/9901023
- [64] T.Barnes, *Z.Phys.* **C10** (1981) 275
- [65] Yu.A.Simonov, Dynamical equations for mesons and baryons, *Phys. At. Nucl.* (in press)
- [66] F.J.Yndurain, Heavy Quarkonium; Lectures at the 1999 Autumn Lisbon School; hep-ph/9910399
- [67] F.J.Yndurain, *The Theory of Quark and Gluon Interactions*, 3d edition, Springer, 1999.
- [68] J. Kuti and V.F. Weisskopf, *Phys. Rev.* **D 4**, 3418 (1971).
- [69] G. Altarelli, N. Cabibo, L. Maiani and R. Petronzio, *Nucl. Phys.* **B 69**, 531 (1974).
- [70] G. Altarelli, S. Petrarca, F. Rapuano, *Phys. Lett.* **B 373**, 200 (1996).
- [71] G. Lepage, S. Brodsky, *Phys. Rev.* **D 22**, 2157 (1980).
- [72] G.'t Hooft, *Nucl. Phys.* **B 75**, 461 (1974).
- [73] M.V. Terentiev, *Sov. J. Nucl. Phys.*, **24**, 106 (1976); P.L. Chung, F. Coester and W.N. Polyzou, *Phys. Lett.* **B 205**, 545 (1988).
- [74] J. Carlson, J. Kogut and V.R. Pandharipande, *Phys. Rev.*, **D 27**, 233 (1983).
- [75] G.B. West, *Phys. Rev. Lett.* **24**, 1206 (1970).
- [76] R.P. Feynman, in *Photon-Hadron interaction*, (Benjamin, New York, 1972)
- [77] P.J. Sutton, A.D. Martin, W.J. Stirling and R.G. Roberts, *Phys. Rev.* **D 45**, 2349 (1992).
- [78] S.I.Kruglov, *Phys. Rev.* **D60** (1999) 116009
- [79] S.I.Kruglov, hep-ph/9910514
- [80] H.G.Dosch, Y.Kripfganz, A.Laser and M.G.Schmidt, *Nucl. Phys.* **B507** (1997) 519

Table 1

Comparison of the WKB spectrum of Hamiltonian (72) $M_n^{(1)}$ with the exact spectrum of Hamiltonian (71) $M_n^{(2)}$ for $m = 0$ and $\sigma = 0.2 \text{ GeV}^2$.

| n | 0 | 1 | 2 | 3 | 4 | 5 |
|-------------|-------|-------|-------|-------|-------|-------|
| $M_n^{(1)}$ | 1.475 | 2.254 | 2.825 | 3.299 | 3.713 | 4.085 |
| $M_n^{(2)}$ | 1.412 | 2.106 | 2.634 | 3.073 | 3.457 | 3.803 |

Table 2

Effective mass eigenvalues $\mu_0(n, l)$ (in GeV for $\sigma_f = 0.18 \text{ GeV}^2$) obtained from Eq.(70), (72) $\mu_0 = \sqrt{\sigma_f} (\frac{a(n)}{3})^{3/4}$ - upper entry, and eigenvalues of reduced equation a(n)-lower entry.

| n | 0 | 1 | 2 | 3 |
|---|-----------------|-----------------|----------------|---------------|
| L | | | | |
| 0 | 0.352 2.3381 | 0.535 4.0879 | 0.67 5.520 | 0.78 6.786 |
| 1 | 0.462 3.3613 | 0.611 4.8845 | 0.732 6.216 | |
| 2 | 0.55 4.248 | 0.68 5.63 | | |
| 3 | 0.627 5.053 | | | |

Table 3

Mass eigenvalues of the rotating string Hamiltonian (67)

| $n \ l$ | 1 | 2 | 3 | 4 | 5 |
|---------|-------|-------|-------|-------|-------|
| 0 | 1.865 | 2.200 | 2.481 | 2.729 | 2.956 |
| 1 | 2.562 | 2.832 | 3.068 | 3.281 | 3.480 |
| 2 | 3.091 | 3.329 | 3.540 | 3.733 | 3.913 |
| 3 | 3.535 | 3.753 | 3.947 | 4.125 | 4.290 |
| 4 | 3.925 | 4.128 | 4.309 | 4.476 | 4.629 |
| 5 | 4.278 | 4.469 | 4.638 | 4.797 | 4.939 |

Table 4

Energy eigenvalue $a(\lambda)$ of the reduced equation (87) as a function of the dimensionless parameter λ , (88); derivative $|a'(\lambda)| = \left| \frac{da(\lambda)}{d\lambda} \right|$ and wave function at origin $\chi_\lambda(0)$ (solution of (87)) divided by $\chi_0(0)$ (solution at $\lambda = 0$)

| λ | 0 | 0.4 | 0.5 | 0.6 | 0.7 | 0.8 | 0.9 | 1 |
|-------------------------------------|-------|-------|-------|-------|-------|-------|-------|-------|
| $a(\lambda)$ | 2.338 | 1.99 | 1.896 | 1.801 | 1.704 | 1.604 | 1.502 | 1.398 |
| $ a'(\lambda) $ | 0.84 | 0.9 | 0.92 | 0.94 | 0.96 | 0.98 | 1.01 | 1.04 |
| $\frac{\chi_\lambda(0)}{\chi_0(0)}$ | 1 | 1.249 | 1.318 | 1.392 | 1.469 | 1.549 | 1.633 | 1.72 |

Table 5

The factor $\rho(AF)$, as a function of parameter λ , (88), for two values of Λ_{QCD} entering (88) via one-loop expression (17)

$$\rho = \frac{\chi_{AF}(0)}{\chi(0)}$$

| $\Lambda_{QCD}; \lambda$ | 0 | 0.4 | 0.6 | 0.7 | 0.8 | 1 |
|--------------------------|---|-------|------|-------|-------|------|
| 90 MeV | 1 | 0.976 | 0.92 | 0.884 | 0.838 | 0.76 |
| 140 MeV | 1 | 0.984 | 0.95 | 0.911 | 0.877 | 0.79 |

Table 6

Mass correction $(-\Delta M)$ in GeV, Eq. (112), due to the rotating string, computed quasiclassically. The entries in parenthesis are obtained from Eq. (113)

| n | 0 | 1 | 2 |
|---|------------------|-------|-------|
| L | | | |
| 1 | 0.082 (0.066) | 0.014 | 0.005 |
| 2 | 0.119 (0.120) | 0.035 | |
| 3 | 0.164 (0.167) | | |

Table 7

Meson masses for the Hamiltonian (85) with the parameters

$$\alpha_s = 0.39$$

$$\sigma = 0.17 \text{GeV}^2$$

$$C_0 = -482 \text{MeV}$$

| meson | mass (theory) in MeV | mass (experiment) in MeV |
|--------------------|----------------------|---|
| $\rho(1S)$ | 769 (fit) | 768.5 ± 0.6 |
| $\rho(2S)$ | 1500 | 1465 ± 25 |
| $\rho(3S)$ | 2035 | 2149 ± 17 |
| $\pi(2S)$ | 1325 | 1300 ± 100 |
| $\pi(3S)$ | 1895 | 1861 ± 13 |
| $\bar{M}(1^3P_j)$ | 1200 | $1230 \pm 22 = M_{cog}(1^3P_j)$ candidates ^{a)} |
| $\bar{M}'2(3P_j)$ | 1790 | $a_2(1700), a_1(1700)$ |
| $\bar{M}''3(3P_j)$ | 2265 | $a_1(2100), a_0(2050)$ |

^{a)} T.Barnes hep-ph/9907259

Table 8

Compilation of lattice results for exotic 1^{-+} hybrid masses (in GeV) compared to calculations of the present approach

| | $M(bbg) - M(bb)$ | $M(\bar{c}cg) - M(\bar{c}c)$ | $M(\bar{s}sg)$ | $M(\bar{u}dg)$ |
|-----------------------|------------------|------------------------------|----------------|----------------|
| Lattice ^{*)} | 1.14[a] | 1.34[e] | 2.00[g] | 1.88[g] |
| | 1.3[b] | 1.22[f] | 2.17[e] | 1.97[e] |
| | 1.54[c] | 1.323[c] | | 1.90[i] |
| | 1.49[d] | | 2.11[f] | |
| Present approach | 1.5 | 1.45 | 2.34 | 2.16 |

^{*)} From D.Toussaint, hep-ph/9909088; [a],...[g] refer to sources in the paper.

Table 9

Lattice data on glueball masses (in GeV) compared to the present approach [60]

| J^{PC} | [61] | [62] | [63] | Present approach [60]($\sigma_f = 0.23\text{GeV}^2$) |
|----------|-----------------|------|------|--|
| 0^{++} | 1.73 ± 0.13 | 1.74 | 1.69 | 1.58 |
| | 2.67 ± 0.31 | 3.15 | 2.48 | 2.71 |
| 2^{++} | 2.4 ± 0.15 | 2.48 | | 2.59 |
| | | 3.22 | | 3.73 |
| 0^{-+} | 2.59 ± 0.17 | 2.38 | 2.54 | 2.56 |
| | 3.64 ± 0.24 | | | 3.77 |
| 2^{-+} | 3.1 ± 0.18 | 3.38 | 3.31 | 3.03 |
| | 3.89 ± 0.23 | | | 4.15 |
| 3^{++} | 3.69 ± 0.22 | 4.31 | 4.27 | 3.58 |
| 1^{--} | 3.85 ± 0.24 | | | 3.49 |
| 2^{--} | 3.93 ± 0.23 | | | 3.71 |
| 3^{--} | 4.13 ± 0.29 | | | 4.03 |
| 1^{+-} | 2.94 ± 0.17 | 3.03 | | |
| 2^{+-} | 4.14 ± 0.25 | | 4 | |
| 0^{+-} | 4.74 ± 0.3 | | | |

Table 10

Characteristics of heavy–light mesons in comparison with experiment and lattice data

| meson | B | B^* | B_s | D | D^* | D_s | D_s^* |
|---|-------|-------|-------|-------|-------|-------|---------|
| $M - m_Q$ | 0.479 | 0.539 | 0.535 | 0.496 | 0.630 | 0.532 | 0.666 |
| M | 5.279 | 5.339 | 5.335 | 1.896 | 2.030 | 1.932 | 2.066 |
| m_{exp} | 5.279 | 5.324 | 5369 | 1.869 | 2.010 | 1.968 | 2.112 |
| $f_M(\text{Gev});$ $\sqrt{\sigma} = 0.427$ | 0.183 | | | 0.221 | | 0.264 | |
| $f_M^{(lat)}$ $\sqrt{\sigma} = 0.427$ | 0.210 | | 0.251 | | | | |

Figure 1: Quasiclassical spectrum of Hamiltonian (67) for $m = 0$ and $\sigma = 0.2\text{GeV}^2$. The leading experimental Regge trajectory in angular momentum L is given in the upper plot for comparison. Theoretical prediction for the ρ -meson mass, with color Coulomb and spin effects included is shown by the dot at $L = 0$ and does not violate the straight-line behaviour of the leading trajectory

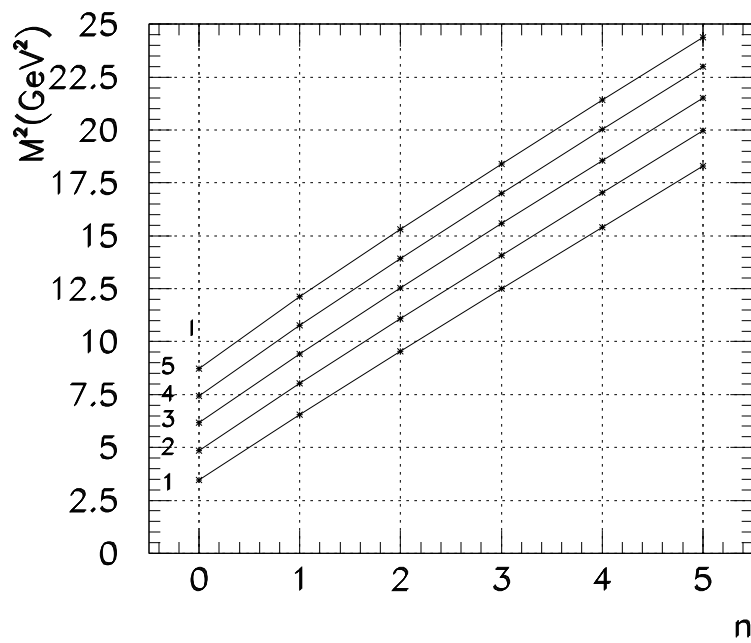
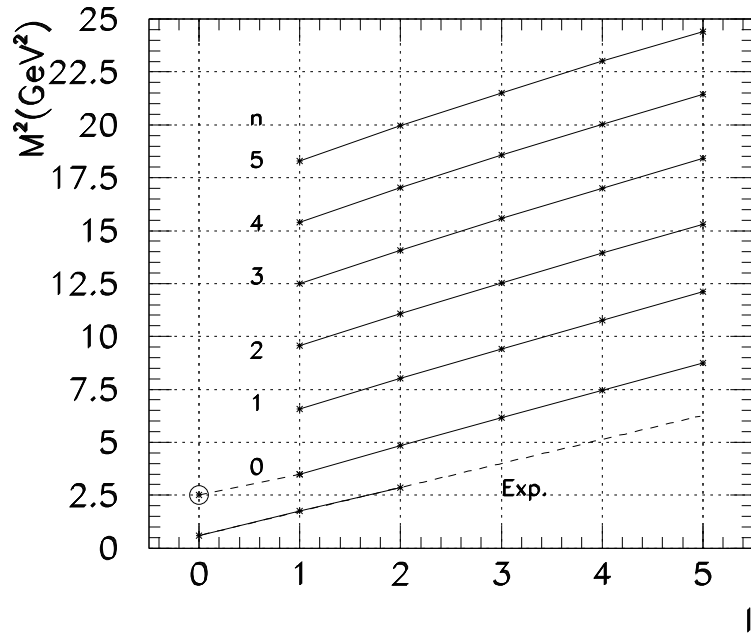
Figure 2: The Chew-Frautschi plot with masses computed via the light-cone (circles, squares and triangle for $L_z = 0, 1, 2$ respectively) and the c.m. Hamiltonian (stars). The systematic overall mass shift is seen as a divergence of straight lines passing through circles and stars. The states with high L or high N_r (daughter trajectories) are numerically less reliable and not shown.

Figure 3: The 3d plots of wave functions of the four lowest states of light-cone Hamiltonian for zero quark masses. Coordinates on horizontal plane are $0 \leq \rho \leq 1$, $0 \leq t \leq 15$ (in units of σ^{-1}).

Figure 4: The same as in Fig. 3 but for heavy quark masses, $m_1 = m_2 = 5 \text{ GeV}$.

Figure 5: The 3d plots of the ground-state wave functions $\Psi(\rho, t)$, computed via the light-cone Hamiltonian (upper part) and via the c.m. Hamiltonian, with the standard substitution (183) (lower part) for zero quark masses.

Figure 6: The quark-distribution function $q(\rho)$ computed with light-cone wave-functions for the cases considered.



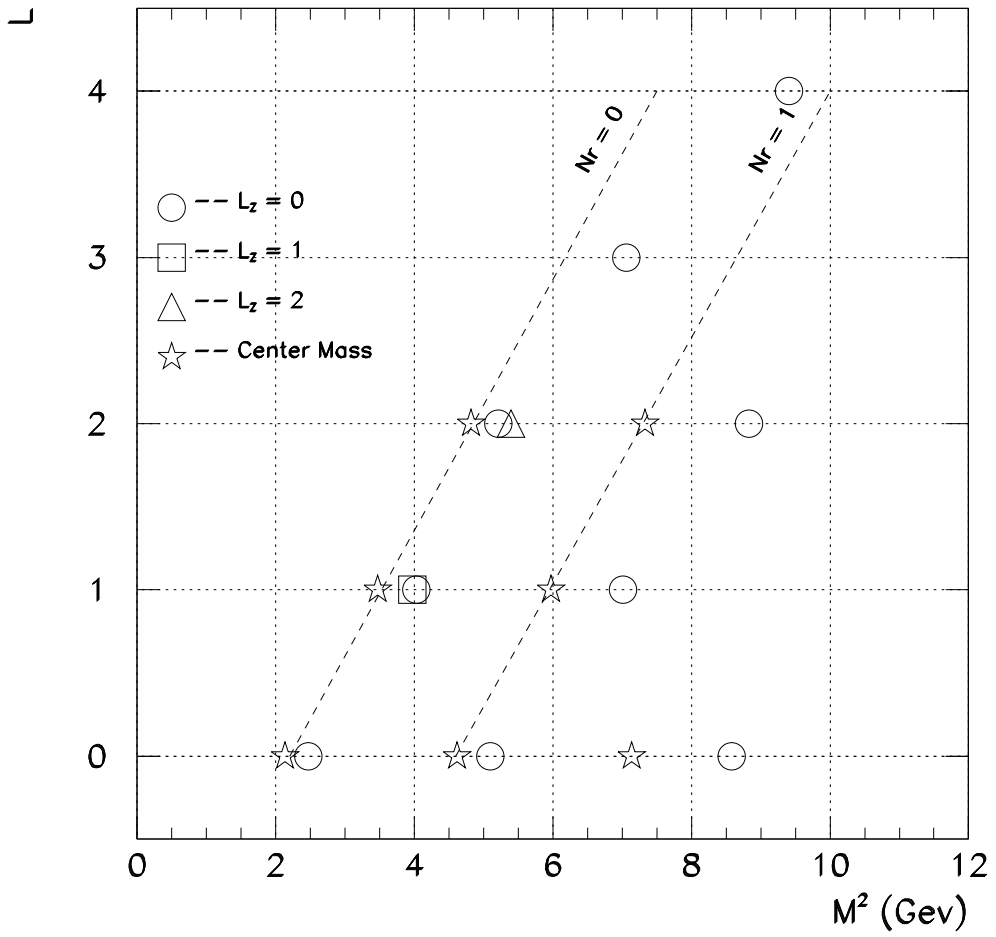


Fig. 1

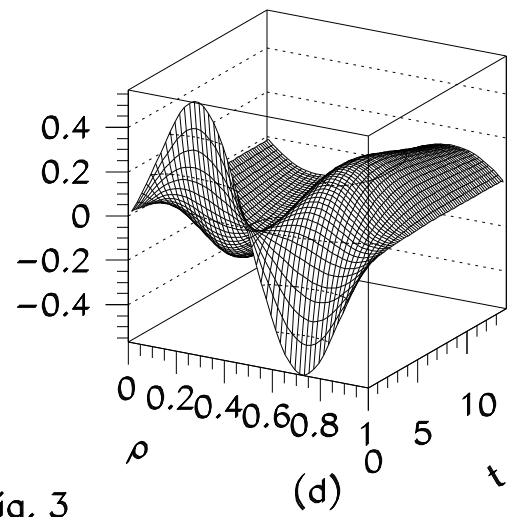
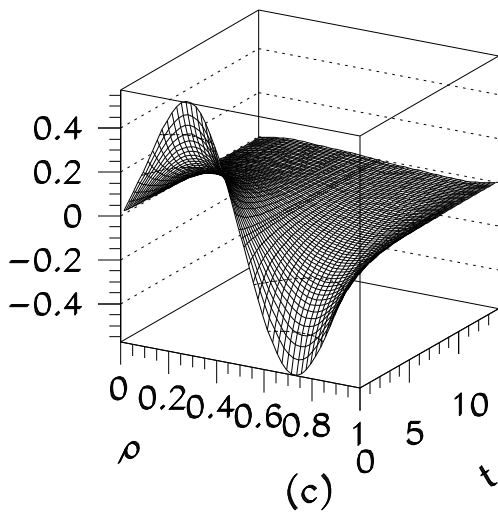
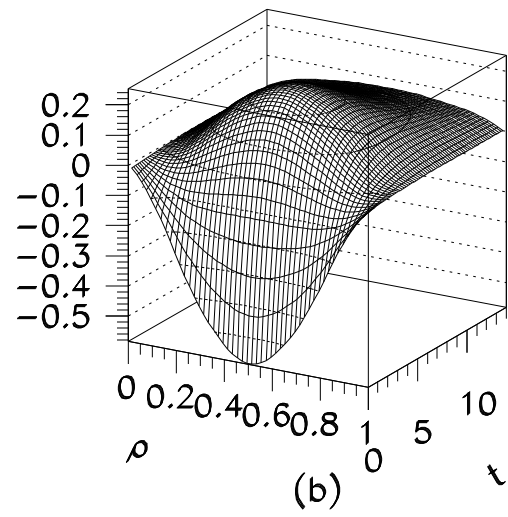
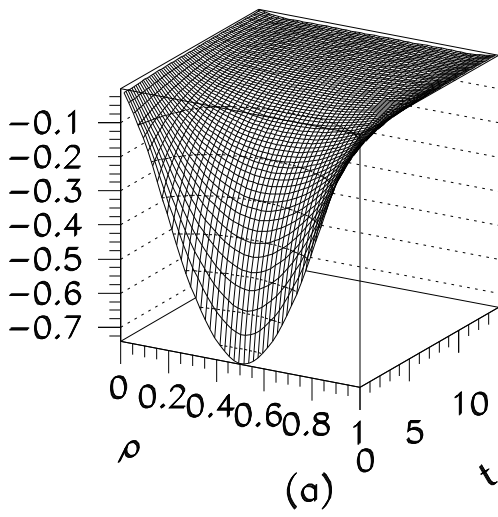


Fig. 3

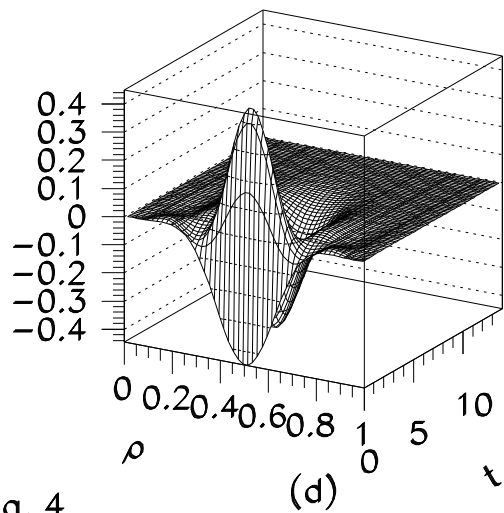
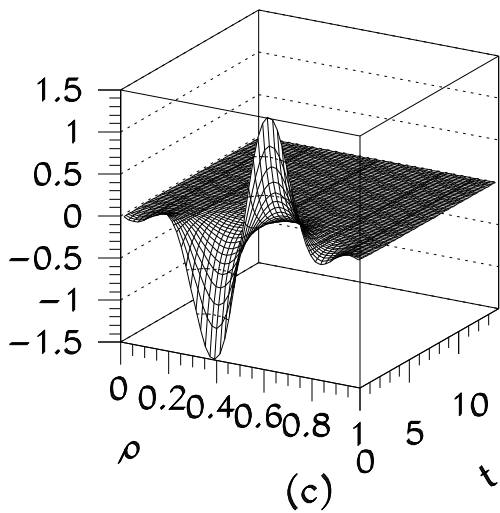
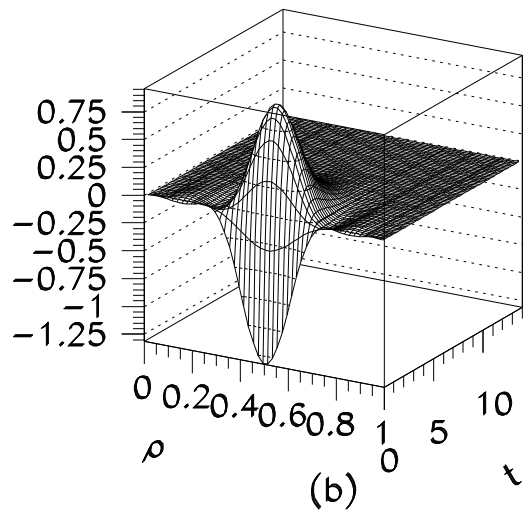
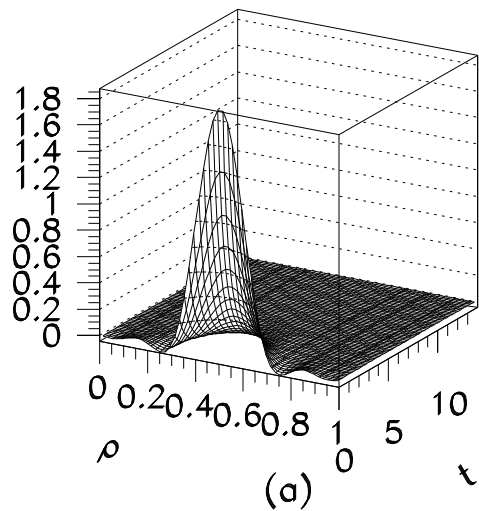
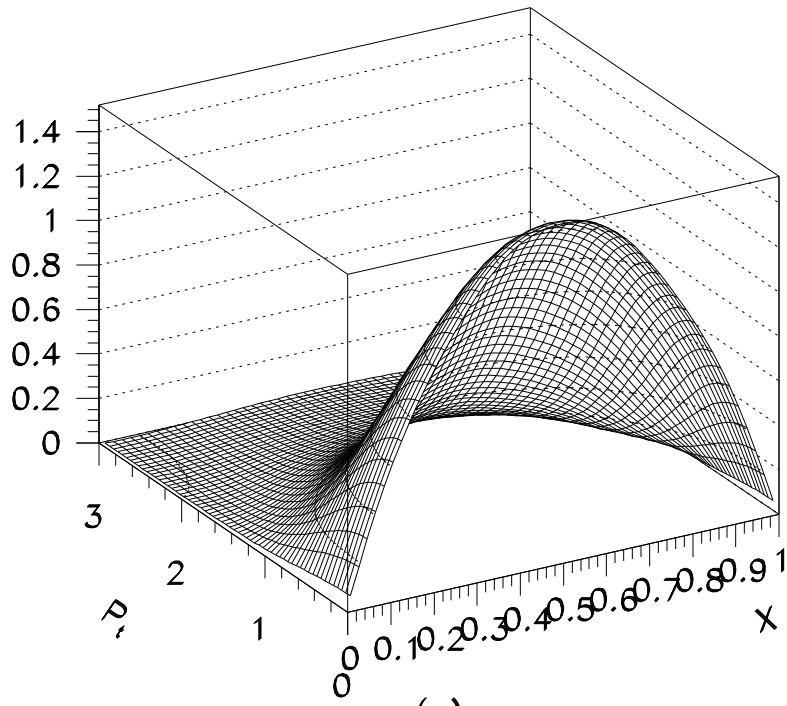
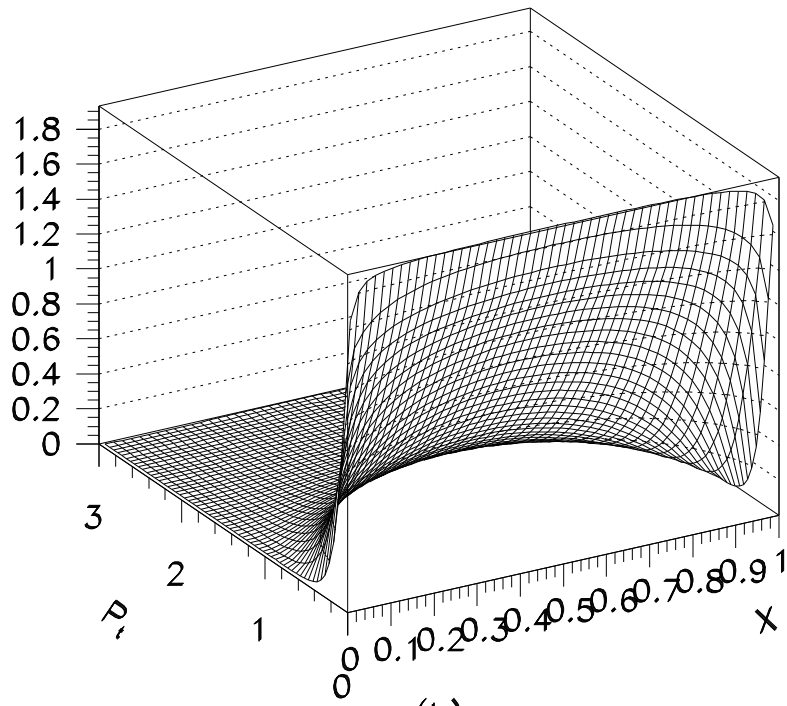


Fig. 4



(a)



(b) Fig. 6

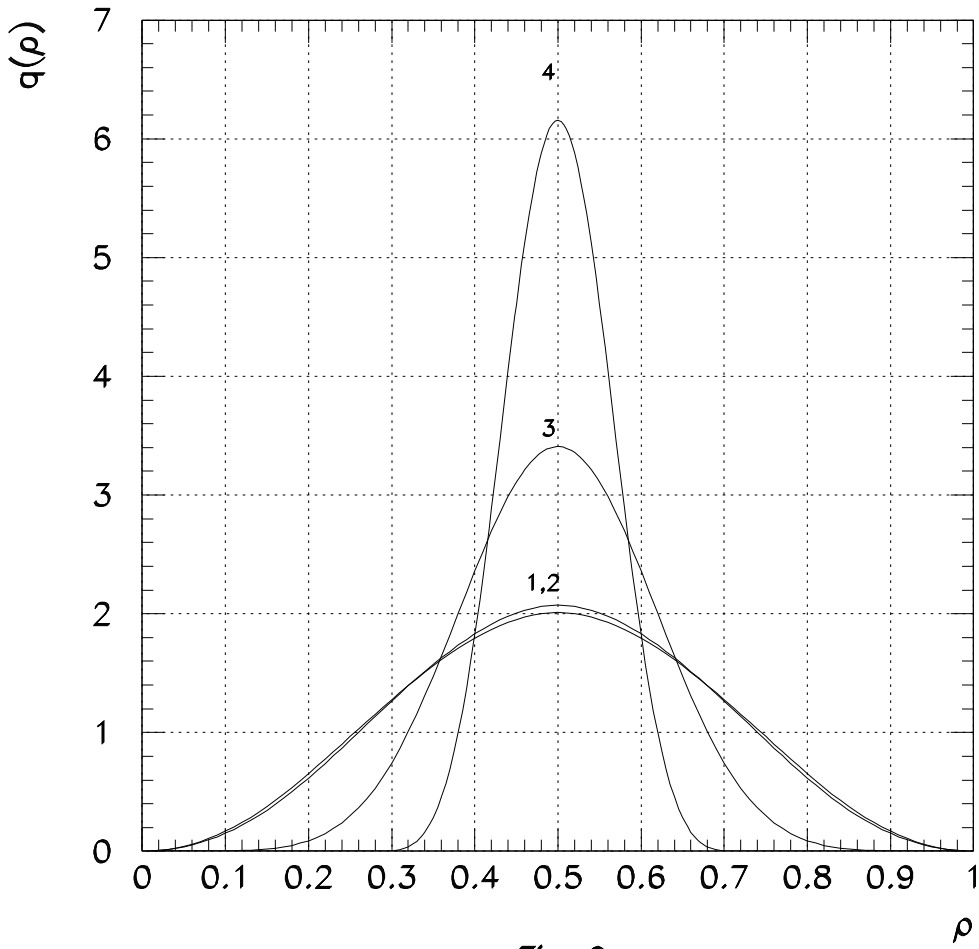


Fig. 9